Journal of Marine Research, 47, 951–992, 1989

A Brownian-pumping model for oceanic trace metal scavenging: Evidence from Th isotopes

by B. D. Honeyman[1] and P. H. Santschi[2]

ABSTRACT

Two observed characteristics of Th isotope and stable metal sorption in natural aquatic systems are seemingly at odds with physico-chemical adsorption theory: (1) characteristic sorption times of days to weeks and (2) K_ds which are inversely related in magnitude to particle concentrations. In addition, sorption rate constants are positively correlated with particle concentrations and K_d.

This paper presents a conceptual and mathematical model with which it is proposed that these metal sorption characteristics have the same underlying physical process in common: the coagulation of colloidal (nonfilterable) particles onto larger (filterable) particles. "Brownian pumping" (the transfer of truly dissolved metal species to filterable particles through a colloidal intermediate) consists of two rate steps: (1) rapid formation of metal/colloid surface site complexes (adsorption) and (2) slow coagulation of colloids with filterable particles. The Brownian-pumping model is tested against field and laboratory data. The field data, obtained from the literature, covers different regions of the oceans: deep ocean environments, euphotic zone, coastal and estuarine systems. The laboratory data involved ^{228}Th sorption in suspensions of goethite and polystyrene latexes. Although the model has general applicability, results and discussions herein emphasize thorium isotope behavior. The Brownian-pumping model suggests that Th or other strongly sorbing elements may be useful as *in situ* "coagulometers" either at relatively high (e.g., greater than 5–10 mg/l) particle concentrations or when the mass ratio of colloids (C_p^*) to filterable particles (C_p) is known. The model also indicates that the ratio of colloids to filterable particles in marine systems, may be, by a first approximation, described by the relationship $\log C_p^* = 0.7 \log C_p - 2.6$ (in units of kg/l).

1. Introduction

It is now widely accepted that adsorption controls the dissolved concentration of a large group of metals. Current adsorption models treat the formation of particle-surface site/metal ion complexes as analogous to the formation of metal-ligand solution complexes, with corrections made for the influence of the electrified interface

1. Environmental Science and Engineering, Department of Civil Engineering, Stanford University, Stanford, California, 94305, U.S.A.

2. Department of Marine Sciences, Texas A&M University at Galveston, Galveston, Texas, 77553-1675, U.S.A.

on complex formation (e.g., Schindler *et al.*, 1976; Hohl and Stumm, 1976; Davis *et al.*, 1978).

Surface complexation theory was first applied to the oceanic scavenging of trace metals by Schindler (1975) and then later expanded upon by Balistrieri *et al.* (1981). Although the work of Morel and Hudson (1986) and Whitfield and Turner (1987) raised some reservations about the general applicability of such an approach, particularly with regard to the role played by the biota, the concept of surface complexation remains a useful starting point for predicting the fate of the group of metals which are predominantly influenced by chemical interactions with particle surfaces (i.e., by "hydrolytic" scavenging).

Scavenging models based upon surface complexation theory are equilibrium descriptions of metal/particle surface partitioning. Such an implicit, *a priori* assumption that adsorptive equilibrium exists was reasonable as, phenomenologically, metal-ion/surface-site complex formation is a ligand-exchange process (protons, or other exchangeable ions, associated with particle surfaces are replaced by metal ions) and, according to physico-chemical theory, the ligand exchange process should be very rapid. Recent kinetic studies of metal-ion adsorption on metal oxides (Hayes and Leckie, 1986; Yasunaga and Ikeda, 1986) have shown that surface-complex formation may be described as a bi-molecular reaction with characteristic formation times on the order of milliseconds. However, characteristic, apparent, sorption times (the average removal time from the dissolved phase to particle surfaces) for metal species in natural aquatic systems range from hours to weeks (10^3 to 10^6 seconds or longer) (Nyffeler *et al.*, 1984; 1986; Honeyman *et al.*, 1988; McKee *et al.*, 1986) indicating that kinetic descriptions of scavenging may be necessary.

The role of colloids in producing slow thorium sorption kinetics was originally postulated by Tsunogai and Minagawa (1978). In their model, dissolved thorium species rapidly and irreversibly adsorb onto colloidal particles; the particles constituting the colloidal size class then reversibly aggregate with larger, filterable particles. Similar, coupled processes have also been hypothesized by Santschi *et al.* (1986), Niven and Moore (1988) and Bacon *et al.* (1985).

Santschi *et al.* (1986) proposed that if the sorption of a metal ion (that is, its appearance in the filterable-particle size class) has particle aggregation as a rate-limiting step, then the rate of sorption should be a function of particle numbers (or particle concentration, C_p). Such dependencies of sorption rate on C_p have been described by McKee *et al.* (1986) and Honeyman *et al.* (1988).

Another observation of metal sorption behavior in which colloids have been implicated is the so-called "particle-concentration effect" in which K_d (concentration in the particulate fraction divided by that in the "dissolved" fraction at equilibrium) decreases with increasing C_p (e.g., Di Toro *et al.*, 1986). Two schools of thought have evolved over the interpretation of these observations. One holds that it is essentially an experimental artifact and the consequence of colloids which are operationally defined

as part of the dissolved fraction but which are never-the-less sorbing solutes (Morel and Gschwend, 1987; Higgo and Rees, 1986). The other set of opinions is that the C_p effect is the consequence of physical/chemical processes (such as particle-particle interactions) affecting the equilibrium particle/solution distribution of solutes (Di Toro *et al.*, 1986; Mackay and Powers, 1987).

Higgo and Rees (1986) and Morel and Gschwend (1987) approach the problem in essentially the same way: the sorption of metals on colloids and filterable particles may be described by characteristic association coefficients for each particle-size group. The dependency of the measured, overall K_d on C_p is due to the relative effect of adsorbates associated with colloids but which are still operationally considered to be in the "dissolved" fraction. Both sets of authors suggest that log K_d is proportional to n log C_p: the exact relationship depends on whether colloids and particles are in a fixed ratio (Morel and Gschwend, 1987; Higgo and Rees, 1986) or are covariant (Higgo and Rees, 1986). Although some of the reported experimental data yields log K_d versus log C_p plots of slope -1, other sorption data is distinctly different (qq.v., Honeyman and Santschi, 1988). For example, ^{230,234}Th (Honeyman *et al.*, 1988; McKee *et al.*, 1986) and ^{7}Be (summarized in Honeyman and Santschi, 1988) isotope data yield plots with slopes (n) between -0.4 and -0.6 and covering a range of over six orders of magnitude in C_p.

a. Evidence for the importance of colloids. The role of submicron-sized particles in affecting the behavior of particle-reactive solutes has long been recognized, although the evidence in many instances has been indirect. Colloid transport through porous media has been reviewed by McDowell-Boyer *et al.* (1986) and the literature on the formation and properties of radiocolloidal dispersions summarized by Kepàk (1977).

Buddemeier and Hunt (1988) studied radionuclide transport in groundwaters pumped from a nuclear bomb test cavity and found that the transition and lanthanide radionuclides, which moved considerably farther than expected from ^{3}H and other conservative species, were essentially all associated with the colloidal (<0.2 μm) fraction. Sheppard *et al.* (1980) concluded that much of the mobility of radionuclides in soil waters is probably due to soil particles in the 2–5 nm range.

Niven and Moore (1988) examined the partitioning of ^{234}Th among dissolved, colloidal and particulate fractions and found that up to 64% of total ^{234}Th was associated with the colloidal (1 nm–0.2 μm) size fraction. Nash and Choppin (1980) estimated that in natural waters at 0.1 mg l^{-1} DOC (humate = 4×10^{-7} eq l^{-1}) the ratio of [ThHu]/[Th_{diss}] would be about 4×10^{10}.

Sequential filtration and ultrafiltration experiments by Santschi *et al.* (1987; 1983) have shown that radioisotopes of particle reactive elements are involved in dynamic cycles of aggregation and disaggregation of colloids in the water column of coastal marine ecosystems while Buchholtz *et al.* (1986) demonstrated the aggregation of colloidal radionuclides in laboratory batch experiments using marine sediments.

b. Objectives. In this paper we present a phenomenological and mathematical model coupling adsorption with colloid aggregation and compare model results to laboratory and field data. For reasons made clear later, we call this a Brownian-pumping model. This paper contains three main sections: (1) results from ^{228}Th laboratory sorption experiments using goethite (α-FeOOH) and polystyrene latexes; (2) the development of the Brownian-pumping model; and (3) the application of the model to our laboratory data and data sets extracted from the literature.

The Brownian pumping model provides a mechanistic explanation for (1) slow sorption rates; (2) sorption rates which are functions of C_p; (3) the "particle concentration effect"; and (4) correlations between sorption rate and equilibrium K_d (e.g., Jannasch *et al.*, 1988). The model yields a means by which Th isotope data may be systematically extended to understanding the behavior of other particle-reactive metals (e.g., Santschi *et al.*, 1980).

c. Note on terminology. An aqueous solute reacts with a pre-existing solid phase by three main processes: adsorption (the accumulation of matter at an interface without the development of a three-dimensional molecular arrangement, i.e., surface complexation), absorption (the diffusion of an aqueous chemical species into a solid phase) and surface precipitation. The generic term used to describe the removal of a solute from the solution phase to a contiguous solid phase by one or more of these processes is *sorption* (Sposito, 1986). Sorption has also been used in a more general fashion to describe the scavenging of solutes from standing bodies of water. "Scavenging," in this context, is even more vague as it may also include active biological uptake.

In this paper we describe the coupling of two processes, coagulation and adsorption, to account for the removal of trace metals from the dissolved phase onto filterable particles. Although sorption is specifically defined as composed of only the three aforementioned processes no other term exists to describe the net result of coagulation coupled with adsorption. Since the mass of "pre-existing" particles is operationally defined by either particle setting, filtration or centrifugation, sorption is used here to also include the aggregation of colloids, and their sorbed metals, with filterable particles. Thus, it is not used in the more rigorous manner suggested by Sposito.

Colloids are particles submicron in size (0.5 nm–0.5 μm) which are suspended in a continuous medium and which have physical/chemical properties different from that of the bulk medium. A colloidal suspension is stable in the sense that the colloids are not easily separated from the bulk medium. For aqueous suspensions, the usual methods of separation are sedimentation, centrifugation or filtration. *Filterable-particles* means those particles removed by filtration (American Heritage Dictionary, Definition #1); it is also meant, here, to more generally include those particles readily separated by some technique from the bulk solution.

Dissolved has a strict thermodynamic meaning. When used in an operational

context (e.g., that portion of a mixture which passes through a filter) it is surrounded by quotes.

The symbol 'K' is reserved for the equilibrium value of a relation among concentrations or activities and 'Q' for nonequilibrium descriptions. The use of K to describe the solution/particle partitioning of a metal (i.e., for K_c^* and K_{pc}) does not indicate that we are attempting a thermodynamic description since we are not relating K to state functions (e.g., ΔH° or ΔS°). However, they are intended to be conditional constants which may, in principle, be corrected for non-idealities (e.g., ionic strength, side reactions) to become intrinsic surface complexation constants.

Appendix A contains a list and the definitions of all variables discussed in this paper.

2. Laboratory studies: ^{228}Th adsorption on goethite and polystyrene latexes

Laboratory studies were carried out to examine the effect of particle concentration on sorption rate and K_d under controlled conditions. Two different sorbents were used in the experiments: polystyrene latexes and goethite (α—FeOOH). The latexes were selected to produce a heterogeneous system with adsorbent properties as near the ideal as possible: uniform, nonporous particles within a narrow diameter range and stable, with respect to coagulation, under the solution conditions of interest. Therefore, diffusion-controlled reactions at the surface should have been minimal. Goethite, in contrast, was chosen as being representative of natural metal-oxides; it also formed unstable suspensions.

a. Materials and methods. Polystyrene latexes were purchased from Interfacial Dynamics Corporation (Portland, Oregon, USA) and arrived suspended in distilled water. The latexes have sulfated surface sites ($\sigma = 4.49\ \mu C\ cm^{-2}$; 357 Å^2 per charged group; specific surface area $= 7.55 \times 10^4\ cm^2\ g^{-1}$ and with a diameter of $0.753 \pm 0.022\ \mu m$) and have an initial particle number of approximately 3.4×10^{11} particles per milliliter. Particles are reported by the company to be stable to 0.25 M of a 1:1 electrolyte solution at pH 7.

The goethite was manufactured in-house using standard procedures. Particles were rod-shaped with average dimensions of approximately $0.02\ \mu m \times 0.1\ \mu m$ with a maximum number of exchangeable sites, as measured by fluoride adsorption, of 4.0×10^{-4} moles/g goethite. Goethite was stored as a slurry at a concentration of $\sim 10^{-3}$ kg/l.

The ^{228}Th ($t_{1/2} = 1.92$ y), purchased from Amersham Corp., was radiochemically pure. Experimental ^{228}Th activities were approximately 5×10^4 dpm l^{-1} ($\approx 10^{-15}$ M). Samples were counted with a Packard Tri-Carb liquid scintillation counter using Insta-Gel as the scintillation cocktail.

The following experimental protocol was used in the ^{228}Th kinetic studies. Teflon beakers were pre-equilibrated with 200 ml of a $^{228}Th/0.05$ M $NaNO_3$ solution at pH 8 for a period of several days before the addition of the adsorbent. In replicate sets of experiments, the pH was adjusted to pH 8 either with TAPS (N-[Tris (hydroxy methyl) methyl)]-3-aminopropane-sulfonic acid) or with a Metrohm Model 645 Dosimat in the pH-stat mode using dilute base. Both systems produced essentially the same rate results. ^{228}Th uptake onto beaker walls was initially very rapid followed by a period of extended, slow uptake after approximately 12 hours. At this point, about 50 to 70% of the initial ^{228}Th was wall-adsorbed and at least 85% of this, irreversibly. Appropriate aliquots of adsorbent stock suspension were then added and, after about 30 sec. of mixing, the initial slurry sample was taken for the kinetic analysis. Total ^{228}Th activity ("dissolved" + particulate) remained essentially constant for the latex systems throughout the course of the experiments indicating no further uptake of Th (either dissolved or colloidal) by beaker walls. The goethite experiments showed the characteristic coagulation → sedimentation behavior described by Farley and Morel (1986): constant total ^{228}Th activities for some period followed by a rapid decrease as particle aggregates sedimented out (qq.v., Section 3e).

Each sample point consisted of total, "dissolved" and particulate ^{228}Th activities. Slurry samples were filtered immediately after removal from the teflon reactor. Filterable ^{228}Th constituted "particulate" Th and what passed the filter was "dissolved." ^{228}Th slurry activities were considered to be total ^{228}Th. Filter assemblies consisted of 10 mm, 0.2 μm pore size Nuclepore filters in Nuclepore Pop-Top Holders. Filters were analyzed for ^{228}Th activity by being placed in the bottom of scintillation vials with a mixture of ^{228}Th-free electrolyte solution and Insta-Gel poured in to fill the vial. Samples were stored for approximately one month to allow the complete ingrowth of daughter products. Separate experiments showed no loss in activity upon storage due to the possible escape of ^{220}Rn gas from the vials.

^{228}Th mother and daughter total α and β activity was measured with a Packard Tri-Carb with a wide window setting at 60% gain. The sum of dissolved and particulate ^{228}Th activities generally agreed with total activities to within 5%, with latex experiments giving consistently better agreement compared to those for goethite.

Goethite colloid analysis: reductive dissolution of iron colloids in the filtrate using equal proportions of filtrate, 0.1 M $Na_2S_2O_4$ and 0.1 M oxalate with measurement of Fe(II) by the phenanthroline method.

All labware coming into contact with ^{228}Th solutions (including filter holders, pH probes, syringes) were checked for ^{228}Th adsorption and were found to be minimal for the time of contact. However, the Nuclepore filters adsorbed 5–10% of the ^{228}Th from solution and solution/particle partitioning and rate calculations were corrected for this ^{228}Th sink.

b. Results. ^{228}Th sorption onto polystyrene latexes as a function of time is shown in

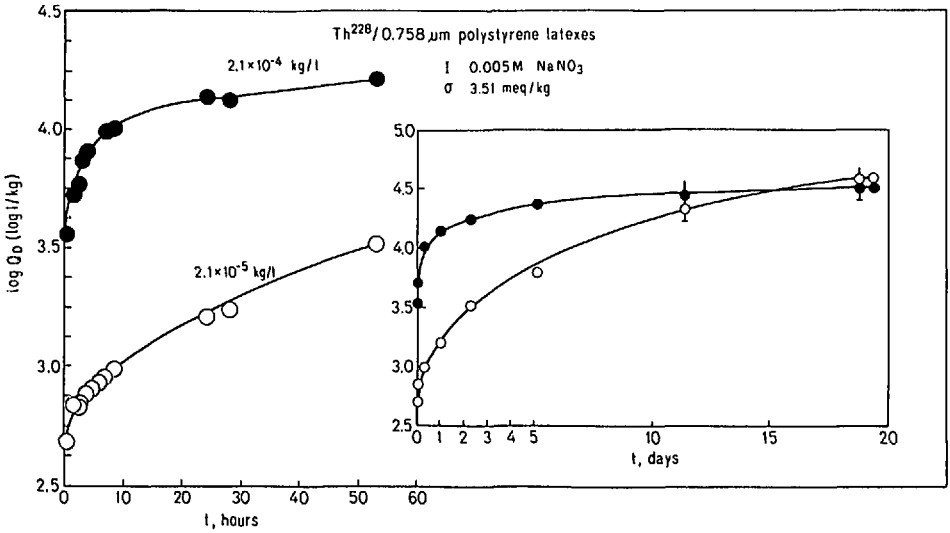

Figure 1. ^{228}Th adsorption on sulfated (0.758 μm) polystyrene latexes: log Q_d(l kg^{-1}) versus time. Ionic strength = 0.05 M $NaNo_3$; pH = 8.0. Particle concentrations: open circle = 2.1 × 10^{-5} kg/l; closed symbol = 2.1 × 10^{-4} kg/l.

Figure 1. Q_d represents nonequilibrium particle phase/solution phase partitioning operationally-defined using 0.2 μm filters. Four characteristics of Th sorption shown in Figure 1 are representative of other published data sets (e.g., Li *et al.*, 1984; Nyffeler *et al.*, 1984): (1) a rapid, initial uptake followed by an extended period of slower sorption; (2) nonzero Q_d values at t = 0 indicating "instantaneous" sorption; (3) a reciprocal relationship between C_p and K_d($Q_d \rightarrow K_d$ as t becomes long); and (4) the rate of sorption increases with C_p.

Observations 3 and 4 are illustrated again in Figure 2 for ^{228}Th sorption onto goethite (α-FeOOH). Figure 2a shows the log of dimensionless loss of nonfilterable ^{228}Th (<0.2 μm) as a function of time. The approach used in the kinetic analysis is given in Appendix C. Sorption data linearized in such a fashion indicate that ^{228}Th removal behaves first order with respect to "dissolved" metal concentration at a particular (fixed) particle concentration. Increasing C_p increases the rate of ^{228}Th removal from solution, as indicated by the slopes of the regression lines. For particle concentrations of 2.1 × 10^{-7}, 2.1 × 10^{-6} and 2.1 × 10^{-5} kg l^{-1}, the rate constants, k_f, are 0.036, 0.2 and 0.44 hr^{-1}, respectively. Figure 2b shows log K_d versus log C_p: the decrease in K_d with increasing C_p is characteristic of the particle-concentration effect.

3. Development of the coagulation model for metal sorption

The model for metal sorption which we are proposing to unify observations of metal behavior couples two processes; adsorption and colloid aggregation. The coagulation

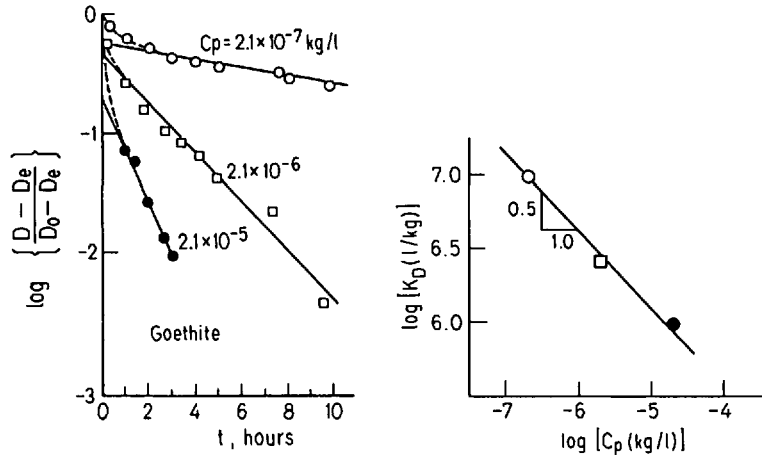

Figure 2. ^{228}Th adsorption onto goethite. (a) log extent of approach to equilibrium versus time and particle concentrations. D, D_o and D_e represent "dissolved," initial and equilibrium ^{228}Th activities, respectively; (b) log k_d(l kg^{-1}) *versus* log C_p(kg l^{-1}). Ionic strength = 0.05 M $NaNO_3$; pH = 8.0.

model for metal sorption describes the transfer of truly dissolved metal species to a filterable-particle fraction via a colloidal intermediate. The particle aggregation mechanism emphasized is Brownian coagulation. The coagulation model is shown schematically in Figure 3. In this, the simplest case, particles in the water column are represented by two particle-size classes: large, filterable particles and smaller, nonfilterable or colloidal particles. The overall transfer of a metal ion from the dissolved state to the filterable particle-size fraction consists of two rate steps:

a. Rapid adsorption. In the first step, dissolved metal species, e.g., Me^{z+}, rapidly form complexes with surface sites on both colloidal and filterable particles; this step most likely has characteristic times, τ_f, on the order of milli-seconds to minutes (Fig. 3a). Consequently, chemical equilibrium is quickly reached and may be described by association constants for large and colloidal particles, K_{pc} and K_c^*, respectively (Fig. 3b). In this paper we are distinguishing between apparent association constants, i.e., K_{pc} and K_c^*, which, in principle, can be directly related to intrinsic (i.e., thermodynamic) complexation constants, and distribution coefficients, K_d and Q_d, which are only effective association coefficients as the "dissolved" (nonfilterable fraction) contains both truly dissolved metal species as well as those associated with colloids. Although it is likely that the apparent association constants of differently-sized particles will be dissimilar (e.g., particle surface-free energy is a function of particle size) there is no direct experimental evidence that they are.

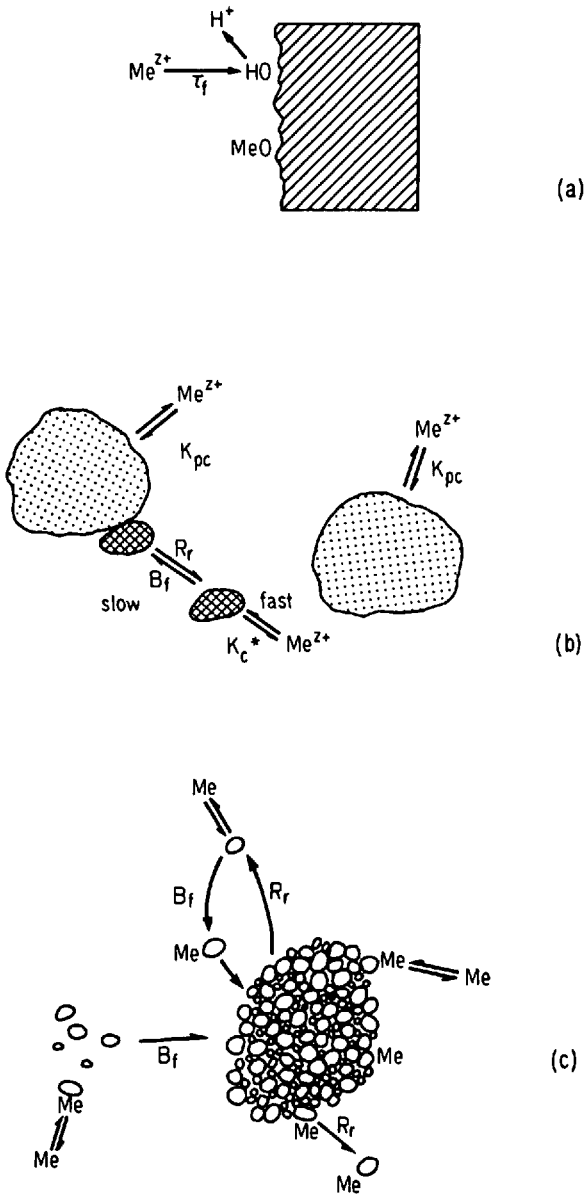

Figure 3. Phenomenological model of coagulation coupled to adsorption consists of two steps: (a) Rapid formation of metal (Me^{z+})/particle surface site complexes with characteristic complex formation times (τ_f) are on the order of 10^{-3} to 10^{-2} sec; (b) Slower aggregation of colloids onto larger, filterable particles. K_{pc} and K_c^* are the metal solution/particle distribution coefficients for filterable particles and colloids, respectively; (c) Natural particle cluster.

b. "Slow" particle aggregation. Colloidal (submicron or nonfilterable) particles slowly aggregate with larger, filterable particles, becoming part of the filterable particle-size class. Particles aggregate and disaggregate according to rate constants B_f and R_n, respectively (Fig. 3b). Most likely, the particles that constitute the filterable particle-size fraction consist of clusters of large and small particles, of varied history and composition, aggregated together (Fig. 3c) and subject to continual reworking. As the solid components of particle clusters gradually make their way to the ocean floor, metal species associated with colloids may periodically cycle through the submicron pool as particle clusters aggregate and disaggregate as the consequence of hydrodynamic forces and biological activity.

c. Particle aggregation. The general dynamic equation for particles in flow systems is described by Friedlander (1977) and Jeffery (1982) and consists of terms for advection, Brownian diffusion and turbulent diffusivities, settling of particles, the increase and decrease of particle numbers in certain size classes as the consequence of coagulation and particle breakup.

Current coagulation theory has as its base the work of Smoluchowski (1917). Coagulation mechanisms are ways in which particles are brought together. The mechanisms, on which a large body of literature exists for aerosol aggregation, have been verified by a number of authors for aqueous systems (e.g., Hunt, 1980; 1982). McCave (1984) described five different coagulation mechanisms and assessed in detail their relative effectiveness for coagulation in the deep sea. The mechanisms are: Brownian motion, laminar and turbulent shear, turbulent inertial coagulation, differential settling and biogenic aggregation processes.

In Brownian coagulation, particles are brought together by the random collisions with molecules in the surrounding medium. "Brownian pumping" is the process by which submicron particles are transferred into larger aggregates and thereby move up the particle size spectrum. In Smoluchowski's treatment, the rate at which particles are brought together by Brownian diffusion is proportional to the square of the number concentration of particles.

The particle size at which the dominant coagulation mechanism changes from Brownian to shear depends on the shear rate: as the rate of shear increases, the critical particle diameter decreases. For oceanic conditions, the particle-size transition region is between 1.5 and 8 μm (McCave, 1984).

Turbulent inertial coagulation is produced when local turbulent accelerations produce relative velocities for particles of unequal mass. This mechanism is relatively unimportant for particles with diameters much less than 1 cm and, therefore, inconsequential for most particles in the oceans.

Coagulation by differential settling is produced as larger, faster particles collide with slower settling particles. The formation of aggregates by this mechanism is a combination of diffusive and collision capture. Differential settling is relatively more

important for large particles and the efficiency of capture by collision increases as the sizes of the catching and caught particles become closer.

Particle aggregation by biota will likely have a significant impact on the particle size spectra in the upper layers of the ocean and McCave (1984) suggests that it is possible to write a coagulation kernal based upon the volume of water swept or filtered. What is unclear, however, is the extent to which particle catching and aggregate production by animals will affect the transfer of submicron particles into larger clusters. Most likely, their major effect relative to inorganic processes will lie in perturbing the population of relatively large (micron-sized or greater) particles.

d. Particle concentration as a master variable for coagulation. No general analytical solution exists for the general dynamic equation coupling coagulation with sedimentation: it must be solved using either simplified analytical solutions (e.g., Hunt, 1982) or numerically. A critical aspect is the solution to the coagulation terms. One approach is to use similarity transforms that reduce the coagulation equation to a function of one independent variable. A characteristic of this approach is the assumption that the particle-size distribution is "self preserving." Such a distribution is one in which a coagulating suspension, after a long time of evolution, develops a particle size distribution whose shape is related to the mechanism governing coagulation.

There are several problems with applying this approach to natural systems. First, particulate matter must be conserved (i.e., no input or removal of particles by processes other than coagulation: e.g., sedimentation, advection, dissolution/precipitation). Second, oceanic conditions are (at least in surface waters) not constant on the time scales needed for the full evolution of the particle-size distribution. And third, similarity transforms will likely fail to describe actual distributions when multiple coagulation mechanisms are operating (Wang and Friedlander, 1967).

Friedlander (1960a,b) suggested that for systems in which there is a flux of particles through the system, beginning with the production of fine particles and ending with their removal by sedimentation at the coarse end, the particle-size spectrum, at "quasistationary" equilibrium, will exhibit subranges each of which is dominated by a single coagulation mechanism. Hunt (1982) followed this approach by assuming that one coagulation mechanism is dominant in each particle size class and showed that the rate of particle mass removal (sedimentation coupled to coagulation) has a second-order dependence on particle concentration. A critical point of Hunt's work is the assumption that collisions between particles of similar size are most important.

Farley and Morel (1986) tested the mass removal rate law and the similarity approach through a combination of sedimentation studies and numerical simulation over a wide range in mass concentration. Based on their experimental results, they proposed a semi-empirical power law expression which has the form of the overall mass removal expression obtained from similarity arguments (Farley, 1984) but which includes the exponents of the three power laws obtained from numerical simulation. In

keeping with Friedlander's approach, Farley and Morel retain the assumption that the collision functions from Brownian motion, fluid shear and differential settling are additive. Thus, the total rate of mass removal of solids, coagulation plus sedimentation (e.g., mg $l^{-1}d^{-1}$), is

$$\frac{dC_p}{dt} = -B_{ds}C_p^{2.3} - B_{sh}C_p^{1.9} - B_bC_p^{1.3} = \hat{B}C_p \tag{1}$$

where B_{ds}, B_{sh} and B_b are the rate coefficients for differential settling, fluid shear and Brownian motion, respectively, and C_p is particle concentration (mg L^{-1}). One coagulation mechanism is dominant at a given particle concentration. An additional difference between the approaches of Farley and Morel (1986) and that of Hunt (1980, 1982) and Hunt and Pandya (1984) is that Farley and Morel empirically adjust the power law expression derived from similarity to account for the effect of the finest particle sizes on shear and differential settling. In other words, collisions between particles of different sizes are most important. The dominance of large particle/small particle interactions has been demonstrated for colloidal iron by Mayer (1982). An interesting aspect of Farley and Morel's work is that while the rate at which particles are brought together by Brownian diffusion has a second order dependence of C_p, the overall rate of removal of particles from a system, in the region in which Brownian coagulation dominates, is proportional to $C_p^{1.3}$.

Figure 4 shows $\hat{B}$ plotted as a function of particle concentration, C_p, for different shear rates (G). The reason for rewriting the rate coefficients as pseudo-first-order rate coefficients will be clarified later. In Figure 4, the Brownian coagulation regime is characterized by that portion of the line of slope equal to 0.3 and that for shear when the slope is 0.9. At low shear rate, mass removal by Brownian coagulation dominates to approximately 100 mg/l; it is only at significant shear rates that coagulation by shear becomes important. Hunt (1980) proposed that at a shear rate of 3 s^{-1} (which is relatively high) Brownian coagulation will dominate up to approximately 1 μm and shear to about 100 μm in particle size. Farley and Morel indicate that a shear rate of about 0.2 s^{-1} would be required for shear coagulation to have any effect on particle aggregation.

For these reasons, and those described in Section 3c, we will emphasize the Brownian coagulation mechanism in our analysis. However, coagulation by differential settling and shear may be readily included. Accordingly, Eq. 1 may be simplified to

$$\frac{dC_p}{dt} = -B_bC_p^{1.3} (\text{mg } l^{-1}d^{-1}) \tag{2}$$

Eq. 2 consists of the term in Eq. 1 for Brownian coagulation and represents the rate at which particles are removed from the system. If new particles are not introduced at the fine end of the particle size spectrum, the overall particle size distribution will be

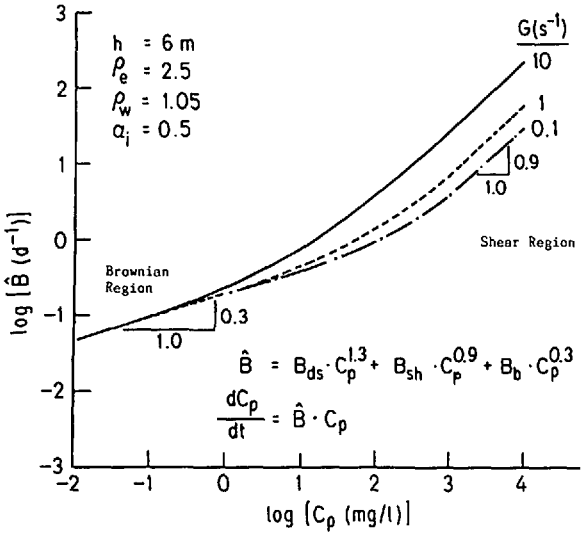

Figure 4. Log of $\hat{B}(\hat{B} = -B_{ds}C_p^{1.3} - B_{sh}C_p^{0.9} - B_bC_p^{0.3})$ as a function of log C_p at various shear rates. A slope of 0.3 indicates the region of Brownian coagulation as the dominant mass removal mechanism.

depleted: small particles by Brownian coagulation and large particles by sedimentation. However, the reduction of the size distribution will be non-uniform as large particles are removed more rapidly by sedimentation than they are replenished by coagulation from the smaller sizes (Farley and Morel, 1986).

Table 1 presents the parameters used in the calculation of $B_b(\text{mg}^{-0.3}\ \text{l}^{0.3}\text{d}^{-1})$ and Table 2 contains parameters used to calculate shear and differential settling kernals and coefficients. The power-law relationships of Eqs. 1 and 2, and the proportionality constant for the Brownian coagulation rate coefficient, B_b, are semi-empirical values which were derived by Farley and Morel through a combination of laboratory studies of batch sedimentation behavior and numerical simulation. The exponents of C_p for the different coagulation mechanisms are representative of characteristic rates of mass removal for different ranges of particle concentration. Eqs. 1 and 2 are nonsteady state descriptions. As will be shown later, a more convenient form of the coagulation rate coefficient is as a pseudo-first order constant

$$B_b' = B_bC_p^{0.3}(\text{d}^{-1}). \tag{3}$$

B_b is, for a particular system, constant, and B_b' has an exponential dependency on C_p. Eq. 2 may be rewritten as a (pseudo) first-order rate expression with respect to C_p

$$\frac{dC_p}{dt} = -B_bC_p^{1.3} = -B_b'C_p. \tag{4}$$

Table 1. Parameters used to calculate the Brownian coagulation coefficient, B_b (after Farley and Morel, 1986).

$$B_b = 1.33(S/h)^{0.6}\rho_e^{-0.3}\,\alpha_b^{0.4}K_b^{0.4} \qquad (\mathrm{mg^{-0.3}l^{0.3}d^{-1}})$$

Stokes settling:

$$S/h = (1/6\pi^2)^{0.33}(g/3\nu h)(\rho_e - \rho_f)/\rho_f \qquad (\mathrm{cm^{-2}s^{-1}})$$

Brownian coagulation kernal:

$$K_b = 2kT/3\mu \qquad (\mathrm{cm^3s^{-1}})$$

Parameter	Description	Dimension	Value*
g	gravitational acceleration	cm s^{-2}	980
ν	kinematic viscosity	$cm^2\,s^{-1}$	0.0098
μ	dynamic viscosity	g $cm^{-1}\,s^{-1}$	0.01
k	Boltzman constant	erg $°K^{-1}$	1.4×10^{-16}
T	absolute temperature	°K	293
ρ_e	particle density	g cm^{-3}	2.5
ρ_f	fluid density	g cm^{-3}	1.025
α_b	collision efficiency factor	(–)	0.1–0.5
h	depth of vertically homogeneous water column	cm	variable

*Values of ν, μ, ρ_e, ρ_f and T reflect typical oceanic conditions.

e. The relationship between submicron particles, C_p^*, and macroparticles, C_p. The phenomenological model of the particle-size spectrum suggested by Friedlander (1960a,b) describes a flux of particles through a system: they start as small particles and end as large aggregates which sediment out of the system. Of course, many particles in natural systems are created rather large only to be broken up and the particle-size spectrum is not necessarily uniform (e.g., log-normally distributed). Never-the-less, very fine particles exist and their relationship in time and space to micron-size particles depends on a complex interdependency of physical and chemical processes.

Table 2. Parameters used to calculate shear and differential settling kernals (K_i) and coefficients (B_i) (after Farley and Morel, 1986).

Shear:

$$K_{sh} = G/\pi \qquad (\mathrm{s^{-1}})$$

$$B_{sh} = 10.0(S/h)^{0.15}\rho_e^{-0.9}\alpha_b^{0.1}K_b^{0.1}\alpha_{sh}^{0.75}K_{sh}^{0.75} \qquad (\mathrm{mg^{-0.9}l^{0.9}s^{-1}})$$

Differential settling:

$$K_{ds} = (6/\pi)^{0.33}(g/12\nu)(\rho_e - \rho_f)\rho_f \qquad (\mathrm{cm^{-1}s^{-1}})$$

$$B_{ds} = 3.12(S/h)^{-0.32}\rho_e^{-1.3}\alpha_b^{0.17}K_f^{0.17}\alpha_{ds}^{1.15}K_{ds}^{1.15} \qquad (\mathrm{mg^{-1.3}l^{1.3}s^{-1}})$$

G has the dimension s^{-1}. Other parameters are defined in Table 1. The subscript "b" indicates a parameter for Brownian coagulation. We assumed that $\alpha_{sh}\,\alpha_{ds} = \alpha_b$.

Eq. 1 describes the net rate of coagulation leading to sedimentation. Consider a closed system composed, initially, of mono-disperse particles (i.e., each particle exists as a discrete entity of size similar to the others). If the particles are subject only to Brownian motion (i.e., they are too small for gravitational settling) and collisions with other particles do not lead to the formation of aggregates, then the particles would stay in suspension indefinitely. Suppose, instead, that a certain number of contacts between particles resulted in the formation of an aggregate. As long as the mass of the aggregate is low its fate will only be influenced by Brownian motions in the fluid, provided that fluid shear rates are small. Although the total mass of the system would remain constant the number of particles would decrease. One would also see a shift in the mass distribution from the pool of singlets to doublets and so on. Eventually, all of the mass would end up in the aggregate pool.

Suppose that by some method one could distinguish between particles of different size. For example, one might select a filter which would collect aggregates of doublet size or greater but which could not retain singlets, the original particles. If C_p^* represents the mass of nonfilterable particles (the singlets) and C_p the mass of filterable particles (doublets, triplets, etc.) then the ratio C_p^*/C_p will change with time. If the system were at steady state, with particle supply and removal in balance, then C_p^*/C_p would be in a fixed ratio, the magnitude of which would be determined by the size limit defining the boundary between the two pools.

At some point the aggregates will become too large to remain in suspension and will sediment out. Assume for the moment that aggregates are still small enough so that their sedimentation does not enhance aggregation. Under such conditions, the formation of aggregates will still be controlled by Brownian diffusion. The term in Eq. 1 for Brownian coagulation thus describes the formation of aggregates by Brownian diffusion and their removal by gravitational settling. The other two terms in Eq. 1 describe the influence of shear and differential settling on aggregate formation and removal rate.

What we are really interested in is the transfer of submicron particles to the filterable-particle pool. If mass is conserved, either in an open system at steady state or in a closed system, then the loss of particles from one pool (i.e., the colloid pool) must be compensated for by a gain in the filterable-particle pool. Thus, although it is currently problematic to measure the loss of particles from the colloid pool (to a large extent this is because the composition of the submicron pool is unknown), we assume that this loss is equivalent to, and can therefore be measured by, changes in the filterable-particle pool. So,

$$-\frac{dC_p^*}{dt} = \frac{dC_p}{dt} = -B_b' C_p. \tag{5}$$

There are two caveats which go with the use of Eq. 5. First, it is strictly appropriate only for systems behaving as batch reactors since it is a description of particle loss:

there is no term for supply. With Eq. 5 we are assuming that the loss of particles from the colloidal particle size class is equal to the gain in mass in the filterable particles size class as particles are transferred up the particle size spectrum and are removed by sedimentation. If the actual particle size distribution is to be maintained at a "quasi-steady-state" then the loss of particles, $B'_b \cdot C_p$, must be balanced in some manner by production. If these particles are submicron in size (or are for the most part) then particle loss must be balanced by their transfer from the submicron pool to the large aggregate pool from which particles are removed from the system. Thus, the rate of production = rate of transfer = rate of removal. Though particle number flux may change in various parts of the spectrum, mass flux should be constant.

The second caveat is that C_p should represent the total particle mass in the system whereas we have defined it in terms of filterable particles. We are assuming that the total particle mass is dominated by particles a few tenths of microns in size or larger, an assumption likely to be true except for environments at very low C_p. Thus, $(C_p^* + C_p) \approx C_p$.

f. Brownian pumping and metal sorption. The rate of transfer of a metal, Me, from the truly dissolved state to the filterable particle size fraction via the population of colloidal particles is dependent on the rate of aggregation of colloids into filterable particles, as described by Eqs. 1–5, and the moles of metal adsorbed per mass of colloids, Γ_c. Thus, with the filterable particle fraction as the reference point,

$$-\frac{dMe_c}{dt} = \frac{dMe_{pc}}{dt} = -\Gamma_c \cdot \frac{dC_p^*}{dt} = -B'_b \cdot C_p \cdot \Gamma_c (\text{mol/l d}) \tag{6}$$

where Me_c and Me_{pc} represent the concentration (M) of metal species associated with colloids and filterable particles, respectively.

Figure 5 is a schematic illustration of the proposed model coupling adsorption and particle aggregation. At low particle concentration, particles are moved up the particle-size spectrum primarily by the Brownian coagulation mechanism. The master variable for the rate of particle-particle interactions is particle concentration (or number concentration). At a particular C_p, the rate at which a metal species is transferred from the truly dissolved state to the filterable-particle fraction is governed by the aggregation rate and Γ_c.

Suppose that the total mass of the metal of interest is distributed among three "pools" (refer to Appendix B for a more detailed treatment of the relationships among master variables): colloids, filterable particles (i.e., particle clusters or aggregates) and solution (i.e., truly dissolved). The fraction of the total metal within each pool is described by f_c, f_{pc} and f_d, respectively. Thus, $f_c + f_{pc} + f_d = 1$. The solution which passes through a filter contains both dissolved metal and metal associated with colloids. The maximum sorption rate which can be expected is achieved when all of the metal in the "dissolved" pool $(f_c + f_d)$ is associated with colloids; that is, when no truly-

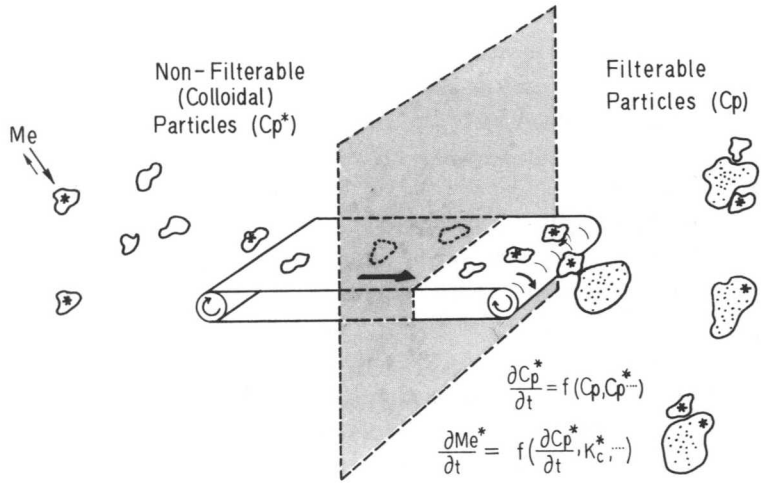

Figure 5. Brownian-pumping: the transfer of dissolved metal to filterable particles *via* a colloidal intermediate. The rate of coagulation of coloidal particles with filterable particles is a function of particle concentration, C_p. The rate of transfer of a metal, Me, from the truly dissolved state to the filterable-particle fraction is a function of the solution/colloid distribution coefficient, K_c^* in addition to the coagulation rate. "*" on particles represents those "tagged" with radioactive metal species.

dissolved metal species exist. Thus, for a given C_p and C_p^*, it is not f_c which is important for estimating the overall sorption rate but $f_{c/d}$, the fraction of metal in the "dissolved" pool associated with submicron particles, and $f_{c/d}$ is a function of only K_c^* and C_p^* (see Appendix B). As $f_{c/d}$ approaches a value of 1, the sorption rate reaches its maximum value: the rate of particle aggregation.

g. Particle disaggregation. Thus far, the discussion has focussed on the aggregation processes. Farley and Morel's (1986) model considers only particle aggregation from an initially mono-disperse state and is a nonsteady-state description. Clearly, for the particle-size distribution to be a steady-state, small particles must be supplied by some mechanism. In Friedlander's concept (1960a,b), fine particle production is balanced by sedimentation. In the oceans, such small particles may be the product of large particle breakup, the erosion of bed material, or other physical, chemical or biological mechanisms.

Authors of conceptual models describing the flux of radionuclides through oceanic water columns have felt the necessity to include aggregate breakup to explain flux patterns. For example, Bacon *et al.* (1985) assume that, although fine suspended matter controls the adsorption of radionuclides, such material does not contribute significantly to vertical fluxes in the ocean. Thus, fine particles are carried downward by a "piggy-back" mechanism (Lal, 1980). Bacon *et al.* argue that aggregation of

small and large particles must occur throughout the water column and that, in order for the population of fine particles to be sustained, disaggregation must occur.

McCave (1984) discussed particle breakup terms for the general dynamic equation for particles. There is relatively little agreement by authors on the functional form of the breakup terms. As is the case with particle aggregation, disaggregation depends in part on the hydrodynamic regime and the composition of the floc; however, no kernals for particle disaggregation have been proposed.

Studies of Th isotope behavior in the water column have pointed to a reversible exchange of Th between the "dissolved" and "particulate" pools. For example, Bacon and Anderson (1982) determined the desorption rate constant (k_{-1}) for ^{230}Th in the deep sea to lie in the range of 1.5 to 4.0 yr^{-1} (4×10^{-3} to 1×10^{-2} d^{-1}); it showed no correlation with C_p. However, the physical meaning of this parameter is unclear. If Th is irreversibly bound as Tsunogai and Minagawa (1978) suggest (or there is significant kinetic hindrance), then k_{-1} may represent the rate constant for particle-cluster breakup into smaller, submicron particles. If Th adsorption is reversible, albeit perhaps slow (Cacheris and Choppin, 1987), then k_{-1} may indicate a combination of bond breaking, pore diffusion and disaggregation.

Moore and Millward (1988) recently studied ^{234}Th sorption in the laboratory using natural marine particles. They proposed that their data could best be described using a serial model composed of three kinetic steps. The desorption rate constant selected for the last kinetic step was 0.05 d^{-1} at 90 mg/l particle concentration. Jannasch *et al.* (1988) also found multiple first-order kinetic steps in laboratory studies of radionuclide sorption by marine particles. Radionuclide uptake was analyzed with both series and parallel reaction schemes and both approaches were found to describe the data equally well. In these studies, the smallest desorption rate constant for ^{230}Th was found to be 0.3 d^{-1} at 1 mg/l.

h. Particle concentration as a surrogate parameter. The master variable C_p, although a convenient measurement, is none-the-less a substitute for more precise parameters. Adsorption is the formation of surface complexes with particle surface sites and dissolved metal species as components. Thus, C_p is a surrogate for site concentration and a relatively imprecise measure at that. For example, marine particulate matter may have specific site concentrations ranging from 0.1 to 10 moles/kg (Balistrieri *et al.*, 1981) while, by comparison, silica may have a specific site concentration as low as 0.01 moles/kg.

Particle mass concentration is also a surrogate for particle number. The likelihood of particles making contact with each other is a function of the number of particles per volume. Since the relationship between particle number and mass concentration depends on the average particle size, two different particle-size distributions, with the same overall C_p, will have different characteristic coagulation times. For example, consider two different particles, each with a different diameter, 0.1 and 1 μm, but of

the same density (2 g/cm^3). If the particles are both present at mass concentrations of 10^{-5} g/l then the number concentrations will be 9.5×10^6 and 9.5×10^3/cm^3, respectively. This difference in particle number concentration represents a three order of magnitude difference in the characteristic coagulation time.

4. Discussion of laboratory studies

a. The effect of particle concentration on sorption rate and equilibrium solution/particle distribution. (i) Latex experiments. It is clear from the behavior of ^{228}Th in the latex suspensions that a relatively slow process is controlling the appearance of the thorium in the filterable-particle pool. The rate of this process depends on the latex concentration. Since latex sites are far in excess of total Th(IV) (even at $C_p = 10^{-5}$ kg/l, [^{228}Th(IV)]/[latex sites] $\approx 10^{-9}$), surface sites could not be limiting and, as such, the fraction of total Th associated with latex surface sites should, for both latex concentrations, be equal and independent of C_p. As a consequence, even if there is a kinetically-hindered redistribution of Th(IV) upon addition of the latex spheres, the time constants should have been the same for both experimental systems. Similarly, one would not expect an increase in mass transport rate with the incremental addition of surface area, with surface area in such great excess. A reasonable alternative is the presence of colloidal impurities.

Consider the ^{228}Th sorption data at a latex concentration of 2.1×10^{-5} kg l^{-1}. Assume, at the time of mixing the ^{228}Th and latex spheres ($t = 0$), that there exists two "pools" of particles: latex particles and colloidal impurities. Assume also that, upon mixing, the thorium instantly adsorbed on particles in both pools. Thus, the "dissolved" ^{228}Th activity at $t = 0$ represents both truly dissolved and colloidal Th. The initial Q_d is not zero because adsorptive equilibrium is achieved at a rate on the order of the mixing time. As time progresses, log Q_d increases because colloidal particles aggregate with latex particles and become part of the filterable particle pool. ^{228}Th sorbs at a faster rate when $C_p = 2.1 \times 10^{-4}$ kg l^{-1} because the rate of coagulation increases with C_p (i.e., the particle conveyor belt of Fig. 5 turns more rapidly). To reiterate, slow sorption is the consequence of fast adsorption coupled to the relatively slow appearance of metal species associated with colloids in the filterable particle fraction.

A peculiar aspect of the sorption data in Figure 1 is that the initial $Q_d(t = 0)$ also increases with C_p. One possibility is that it is an artifact of the filtration process. Such an increase in filter efficiency with particle loading is characteristic of "deep filter" behavior, i.e., the ability of a filter bed (in this case a membrane filter with a relatively high particle loading) to remove particles smaller than the nominal pore size of the filter (e.g., Diamadopoulos and Woods, 1984; Amirtharajah, 1985; Johnson and Wangersky, 1985). The filtration efficiency should increase with filter loading (i.e., C_p).

An additional possibility is as follows. Phenomenological studies of metal sorption (e.g., Li *et al.*, 1972; Jannasch *et al.*, 1988) have shown that sorption rate data may

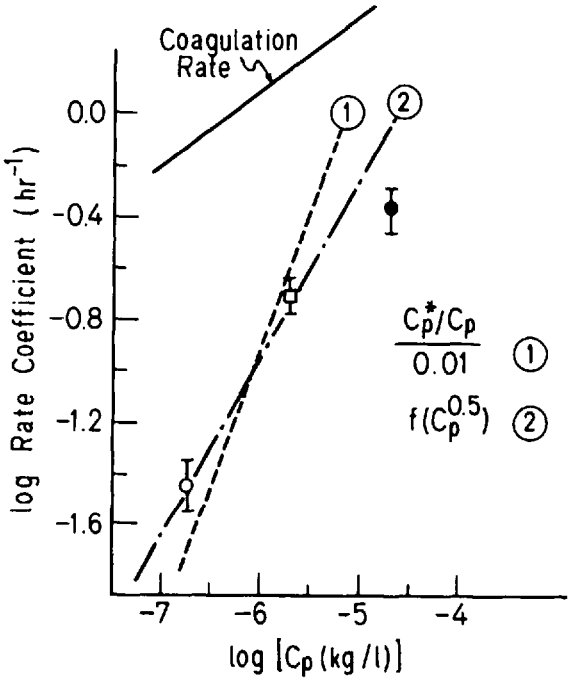

Figure 6. Log rate coefficient, $k_f(\text{hr}^{-1})$, *versus* log C_p for ^{228}Th sorption in the presence of goethite. Rate constants were taken from the data presented in Figure 2. $f_{c/d}$ for Lines 1 and 2 was calculated using $K_c^* = K_{pc} = 10^7$ and the C_p^*/C_p relationships shown in the figure. h = 5 cm.

often be composed of several time regions each of which exhibits first order behavior. These regions may represent, for example, (i) bulk solution mass transport control coupled to adsorption, (ii) coagulation or (iii) absorption. Since the time which elapses before the first measurement is perhaps several minutes (as constrained by experimental procedures), $Q_d(t = 0)$ could represent the extent of an initial, rapid reaction which is dependent on C_p (e.g., *i* or *ii* of the above).

(ii) Goethite experiments. The data in Figure 2 for ^{228}Th sorption onto goethite also indicate that at least two processes with different time constants are operating to affect overall sorption: (1) the *y*-intercepts of the straight line portions of the $(D_t - D_e)/(D_o - D_e)$ versus time curves are nonzero; (2) the intercepts decrease with increasing C_p indicating that there is a particle concentration dependence on the initial sorption process (or processes).

The sorption data shown in Figure 2 represent the time scales of interest for coagulation by Brownian diffusion. The log of the pseudo-first-order rate constants (k_fs) are plotted against log C_p in Figure 6. The solid (uppermost) line is the calculated

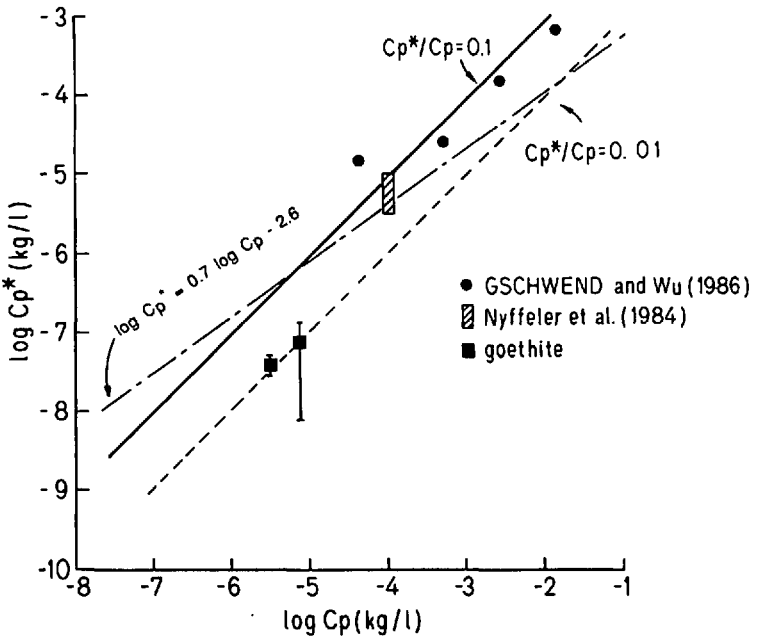

Figure 7. Comparison of filterable (or settleable) particle concentration with that of nonfilterable particles. The data of Gschwend and Wu (1986) is for natural sediments with colloids reported as total dissolved solids (TDS). The symbol representing Nyffeler *et al.'s* (1984) data indicates the range in C_p^* needed to fit the data in Fig. 8. Goethite colloids (those, in this study, passing through a 0.2 μm Nuclepore filter) were determined by reductively dissolving α—FeOOH in the filtrate and analyzing for Fe(II).

removal rate constant (coagulation + sedimentation), B_b' (e.g., Table 1) for the system. The slope of the log B_b' versus log C_p is 0.3 and reflects the relationship: $B_b' = B_b \cdot C_p^{0.3}$ (Eq. 3).

Observed sorption rates are the result of two factors: (1) the rate of particle aggregation and sedimentation and (2) the fraction of metal in the "dissolved" phase actually associated with colloids, i.e., $f_{c/d}$. The sorption rate constant, k_f, is related to the coagulation rate constant by

$$k_f = B_b' \cdot f_{c/d}. \tag{7}$$

The coagulation line is the case for which $f_{c/d} = 1$. An estimation of the appropriate $f_{c/d}$ for a particular system requires a knowledge of C_p^* and K_c^* (qq.v., Appendix B).

C_p is a directly measurable quantity; however, C_p^* is much more elusive to determine. Figure 7 shows measured colloid concentrations as a function of filterable (or settleable) particle concentration. Gschwend and Wu (1985) operationally defined C_p^* as totally dissolved solids (TDS) in their analysis of natural sediments. The goethite colloids of this study were measured through reductive dissolution of iron particles in

the filtrate solutions. The data from Nyffeler *et al.* (1984) are for marine particles and will be described below. The relatively large scatter in the data of Figure 7 and the fact that the particle types range from heterogeneous mixtures of particles (with high DOC) to well-characterized model particles in simple electrolytes makes it difficult to generalize about the relative mass contribution of colloids to micron-sized particles. Nevertheless, Figure 7 provides a useful starting point for estimating the mass contribution of sub-micron particles.

In the coagulation model for sorption, a metal is distributed among three pools: the truly dissolved state and colloidal and filterable particles. In a sense, colloids and filterable particles compete against each other for species of an element. As such, the equilibrium distribution of a metal among these pools is described by Eqs. B1 through B4 (Appendix B). K_d, the apparent distribution coefficient, may be described with the parameters K_{pc}, K_c^* and C_p^* (Eqs. B14 and 17; qq.v., Morel and Gschwend, 1987)

$$K_d = \frac{K_{pc}}{1 + K_c^* \cdot C_p^*}. \tag{8}$$

The values of K_{pc} and K_c^* are independent of C_p and C_p^*, respectively. Thus, Eq. 8 indicates that a plot of log K_d versus log C_p^* should produce two regions of behavior: (1) at low C_p^*, such that $K_c^* \cdot C_p^* \ll 0.05$, K_d will be independent of C_p^* and equal to K_{pc}; (2) at high C_p^*s, K_d will have an inverse dependence on C_p^*. The dependence of K_d on C_p will, in turn, reflect the relationship between C_p^* and C_p. For example, if C_p^*/C_p is constant, a plot of log K_d versus log C_p will have a slope of -1. The plot shown in Figure 2b indicates that C_p^* has a square root dependence on C_p since the data fall on a line of slope equal to -0.5.

Figure 6 shows calculations from the pseudo-first order rate constant k_f as a function of C_p, for (1) $C_p^* = 0.01\ C_p$ and (2) $\log C_p^* = 0.5 \log C_p - 4.6$. Relationship 2 was determined from a combination of the slope of the line in Figure 2b and estimates of the colloid mass in the filtrate (Fig. 7). These particle-concentration relationships were used, with $K_c^* = 10^7$, to calculate $f_{c/d}$ as a function of C_p and, therefore, via Eq. 6, k_f. A comparison of Lines 1 and 2 shows the relative sensitivity of model calculations to assumed relationships between C_p^* and C_p.

In batch experiments such as these, K_d is approached asymptotically as the labeled colloid pool becomes depleted and all submicron particles become part of the aggregate pool. As particles are transferred out of the "dissolved" pool $f_{c/d}$ will gradually decrease until, in the limit, it is equal to zero. Thus, even though the partitioning of a metal between solution and particles (colloids and filterable particles) does not change with time after the initial, rapid sorption, the rate of Brownian pumping will decrease with time because $f_{c/d}$ will decrease (provided no particle disaggregation occurs). Such a reduction in $f_{c/d}$ is a possible source for the multiple rate regions often observed for batch sorption experiments (Jannasch *et al.*, 1988; Li *et al.*, 1972).

Kinetic studies of the adsorption mechanism by Hayes and Leckie (1986) and Yasunaga and co-workers (e.g., Yasunaga and Ikeda, 1986) have demonstrated the second order character of adsorption rate constants. Adsorption, as examined at the observational level of most laboratory and field studies, is the consequence of a number of reactions, including surface protolysis and electrolyte ion/particle surface site interactions. Thus, partitioning and rate constants are conditional (even excluding colloid effects) as they implicitly include a variety of sub-reactions. However, in spite of this complexity, one might expect that microscopic reversibility, applied through a series of consecutive steps, all homogeneous in rate expressions, could yield a second-order character to rate constants at the macroscopic level.

The dependency of k_f on C_p in Figure 6 is clearly not second order, although that does not by itself rule out that the effects are produced by the adsorption step (and the attendant reactions) alone. However, two factors interfere with invoking adsorption as the sole process.

First, goethite size concentrations in the experiments ranged from $\sim 4 \times 10^{-8}$ to 4×10^{-6} M (using a site density for goethite of 220 mmole/kg; Balistrieri and Murray, 1981) while the maximum ^{228}Th concentration of the experiments was $\sim 10^{-15}$ M. As such, given that goethite sites were far in excess of available Th atoms, one would expect that k_f would be insensitive to changes in C_p.

Second, the values of the characteristic sorption times ($1/k_f$) measured in the goethite experiments are orders of magnitude larger than those measured in kinetics experiments examining adsorption mechanisms (e.g., Hayes and Leckie, 1986).

Although it could be argued that Th(IV) has a relatively complex solution chemistry and that exchange among species might kinetically hinder sorption, what has been inferred about Th speciation in simple electrolyte solutions suggests that Th sorption onto metal oxides is similar to that of other hydrolyzed metals. In the introduction to Section 3, we indicated that K_{pc} and K_c^* are surrogate parameters for complexation constants as they implicitly include all reactions (solution and surface) resulting in the adsorption of Th (e.g., surface protolysis, surface site/electrolyte ion interactions, etc.). Hunter *et al.* (1988) have recently reported results for Th adsorption onto goethite in the presence of seawater major ions. At $C_p = 5.4 \times 10^{-4}$ kg/l and $Th_{total} = 9$ μmol, $K_d \approx 10^{3.7}$ (l/kg) at pH 5. Their modelling results (using the model of Davis *et al.*, 1978) suggest the formation of the surface species: SO^-—Th^{4+}[1, 1.0]; SO^-—$ThOH^{3+}$[1, −0.75]; SO^-—$Th(OH)_2^{2+}$[3, −2.38]; SO^-—$Th(OH)_3^+$[4, −9.85]; SO^-—$Th(OH)_4$[5, −16.75]; SO^-—$Th(SO_4)^{2+}$[1, 9.25]. The numbers in brackets are stoichiometric coefficients for proton release and the estimated conditional intrinsic equilibrium constants for the reactions, respectively. If the postulated speciation for thorium proposed by Hunter *et al.* (1988) does in fact exist, rather than more complex polynuclear species, then it is reasonable to assume that Th adsorption onto metal oxides should be relatively fast as is the case for a number of other metal ions.

In contrast, Th(IV) adsorption onto or association with DOC is undoubtedly more

complex than is the case for its sorption onto metal oxides. Nash and Choppin (1980) found that Th(IV)/fulvic acid complexes are very stable as the consequence of a complexation entropy. Cacheris and Choppin (1987) studied the association and dissociation of Th-humate complexes and reported that Th likely binds to (at least) two types of humate sites: those located on the surface of humic acid and others located within the coiled structure. Th formed complexes with the first type of site rapidly and had large dissociation rate constants. In contrast, Th formed complexes with the second type of site very slowly and had small dissociation rate constants. However, Cacheris and Choppin were unable to reconcile the kinetic behavior of Th in concentrated solution with the equilibrium behavior of Th at tracer levels.

b. Sorption rate constants as a function of K_d. Jannasch *et al.* (1988) have shown, by using the laboratory experimental data of Nyffeler *et al.* (1984), that a broad correlation exists between the measured sorption rate constant, k_f, and K_d (Fig. 8a). A theoretical basis does exist for correlations between the rates of approach to equilibrium and the stability constants for a related series of ligand exchange reactions (i.e., Linear Free Energy Relationships: Hoffman, 1982). However, it is doubtful that the k_f values of Nyffeler *et al.* (1984) have any significance on the molecular level. Since K_d represents a ratio of rate constants (irrespective of whatever process or mechanism the constants themselves represent), one would expect that $\partial \log K_d/\partial \log k_f$ would be approximately equal to one.

The Brownian-pumping model suggests also that such a relationship between K_d and the apparent rate constant of sorption should exist. Assume that the rate of particle coagulation is unaffected by the type of metal adsorbed. Given then, that B'_b is constant at a given particle concentration, k_f is proportional to $f_{c/d}$ which in turn is related to K_d (e.g., Eqs. B8 and B14). K_{pc} and K_c^* are the characteristic adsorption *constants* for a specific sorbate and particle type. Variations in K_d (the distribution coefficient) reflect metal-dependent differences in K_c^* and K_{pc}. A high K_d indicates that K_c^* and K_{pc} are also relatively large.

Shown in Figure 8a are the predicted rate constants (given by the Brownian-pumping model using appropriate values of parameters to calculate B'_b) as a function of K_d and for two different ratios of C_p^*/C_p. The range in this ratio is shown in Figure 7 for comparison to measured C_p^*/C_p ratios. The Brownian pumping model reproduces the general relationship between k'_f and K_d; however, given the simple assumptions upon which the model is based, it is unable to account for vertical scatter in the data (particularly with respect to the redox sensitive elements Mn and Co). Figure 8b shows the postulated distribution of the metals as a function of log K_d. Note that it is not the fraction of metal on the colloids, f_c, which is important in producing the observed effect, buf $f_{c/d}$ (Eq. B8). As $f_{c/d}$ approaches 1, the sorption rate constant approaches the limiting rate constant, B'_b ($\sim$1 d^{-1} at $C_p = 10^{-4}$ kg/l).

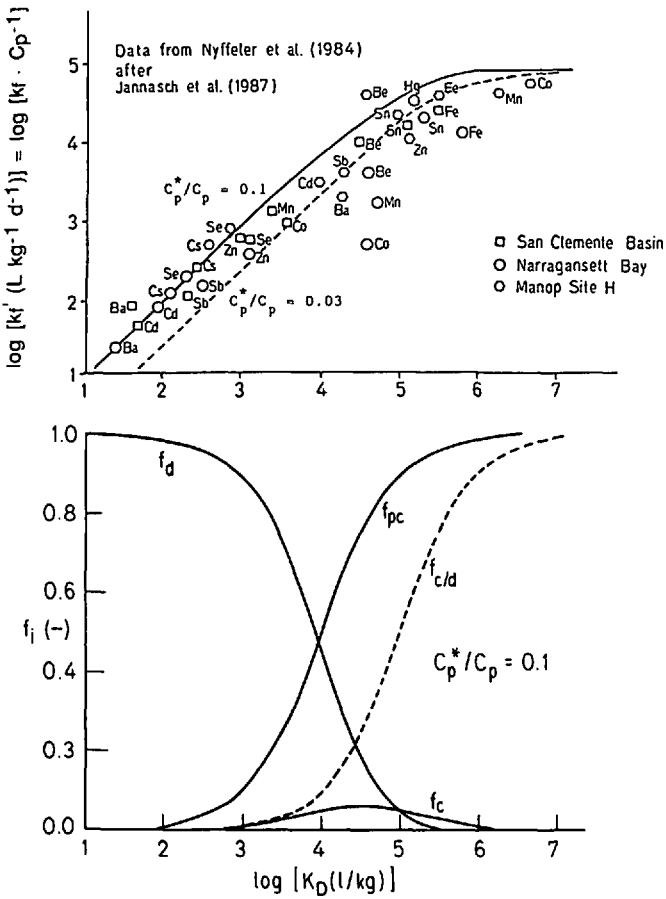

Figure 8. Log sorption rate constant, k_f'(l kg^{-1} d^{-1}; $k_f' = k_f/C_p$) as a function of log K_d(l kg^{-1}). $C_p = 10^{-4}$ kg l^{-1}. Data from Nyffeler *et al.* (1984) after Jannasch *et al.* (1988). k_f' is used instead of k_f(d^{-1}) so that the notation remains consistent with that of the sources. k_f and K_d were determined in the laboratory using sediment material. All values for the computational parameters are the same as in Table 1 with the exception that $h = 5.0$ cm.

5. Brownian pumping and oceanic scavenging

The Brownian-pumping model developed above is a linked combination of rapid metal surface-complex formation and slow particle-particle interaction. In the following section, the model is applied to field and laboratory data and is presented as a hypothesis to explain (i) slow observed sorption rates; (ii) rates which are a function of C_p; and (iii) the reciprocal dependence between K_d and C_p for oceanic Th data.

The current oceanographic paradigm for hydrolyzable metals holds that for a number of metals, metal solubility is controlled by the adsorption of metals onto

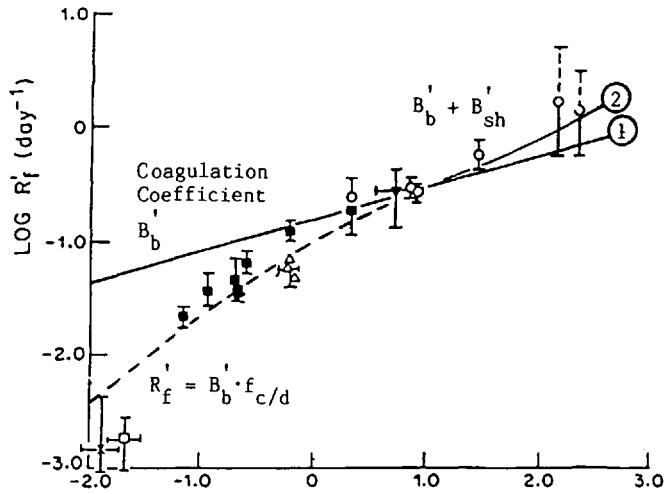

Figure 9. Comparison of the pseudo-first order sorption rate constant, R'_f determined from isotopic disequilibrium (after Honeyman *et al.*, 1987; data from □Nozaki *et al.*, 1987; X Bacon and Anderson, 1983; ■Coale and Bruland, 1985; ○McKee *et al.*, 1984, 1986; △Minagawa and Tsunogai, 1980; ▲Santschi *et al.*, 1979), with calculated Brownian pumping rate constants, as a function of particle concentration, C_p (mg/l). Parameter values as in Table 1 except: $\alpha_b = 0.5$, $\rho_e = 2.5$ g/cm and h = 6 m. (a) Solid lines: (1) Brownian coagulation rate constant (B'_b); $B_b = 1.7 \times 10^{-6}$ l$^{0.3}$ mg$^{-0.3}$ d^{-1}; (2) Brownian and shear coagulation. The solid lines are the cases where $f_{c/d} = 1$ at all particle concentrations. At particle concentrations greater than approximately 5 mg/l, metal scavenging is at the limit defined by particle coagulation. Broken line: $B'_b \cdot f_{c/d}$; $K_c^* = K_{pc} = 10^{7.0}$; log $C_p^* = 0.7 \cdot \log C_p - 2.6$; (b) postulated distribution of ^{230,234}Th for the conditions represented by the broken line in 10a. Symbols are as defined in Appendix A. The fraction of Th in the filterable-particle fraction, f_{pc}, was derived from the sources listed for a.

sinking particles (e.g., Balistrieri *et al.*, 1981; Whitfield and Turner, 1987). A general expression for the rate of "scavenging" of dissolved radiogenic metals by settling particles in a water column (e.g., Bacon and Anderson, 1982; Honeyman *et al.*, 1988) is given by a sum of production and removal rates. With the particulate phase as the reference point, and with ^{234}Th as an example

$$\frac{d[\mathrm{Th_{part}}]}{dt} = R'_f \cdot [\mathrm{Th_{diss}}] - R_r \cdot [\mathrm{Th_{part}}] \pm J(\mathrm{dpm/l \cdot d}). \quad (9)$$

R'_f and R_r represent pseudo-first-order (d^{-1}) adsorption and desorption rate constants, respectively, $\mathrm{Th_{diss}}$ and $\mathrm{Th_{part}}$ are dissolved and filterable-particle radioactivities, respectively, and J represents other production and sink terms for the metal. Sinks include radioactive decay ($\lambda_{\mathrm{Th}} \cdot \mathrm{Th_{part}}$) and the removal of particles by sinking ($\lambda_{\mathrm{part}} \cdot \mathrm{Th_{part}}$).

The data presented in Figure 9 follow from the analyses by Honeyman *et al.* (1988)

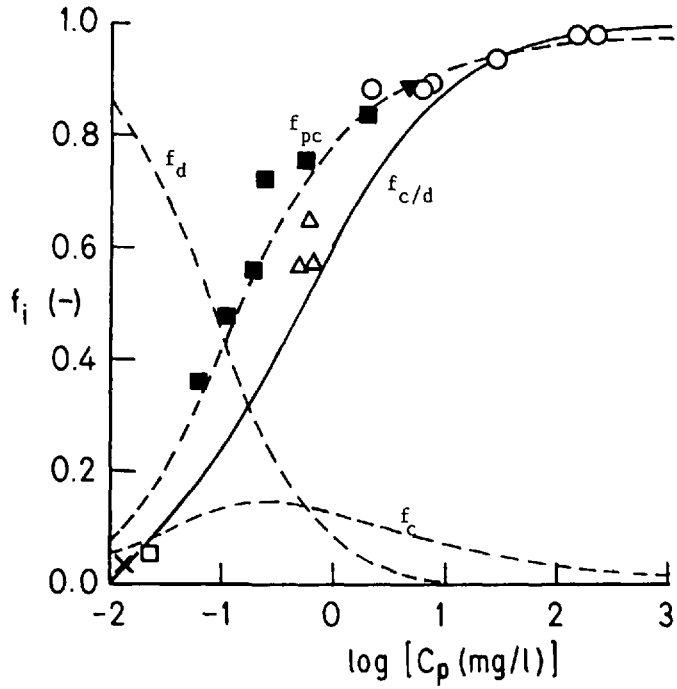

Figure 9. (Continued)

for U/Th disequilibrium in a variety of estuarine and oceanic systems. At steady state, Eq. 9 is equal to zero and the equation may be rearranged to represent R'_f in terms of measurable values:

$$R'_f = \frac{A_{\text{Th part}}}{A_{\text{Th diss}}} (R_r + \lambda_{\text{Th}} + \lambda_p) = R_f \cdot C_p^{\phi} \tag{10}$$

where A represents activity (e.g., dpm L^{-1}).

Figure 9a is a plot of the log of R'_f as a function of log particle concentration. R'_f is not constant but increases with C_p. Characteristic sorption times range from $\sim 10^3$ days in the deep sea to ~ 1 day or less in a high C_p estuarine environment.

The solid lines in Figure 9a represent model estimates for coagulation rate constants, using the parameter values of Table 1 and $h = 6$ m. The selection of a value for h should reflect a mean path scale for a ^{234}Th atom which is associated with sinking particles. Since ^{234}Th has a short half-life the path scale for the deep ocean will be bounded by how far a particle can sink within the average life-time of a ^{234}Th atom (about 35 days). If we consider particles with a mean life of 10 years (Bacon and Anderson, 1982) settling over a depth of 4000 m, one can estimate an average particle sinking rate of about 1.1 m/d. Given an average ^{234}Th atom life of about 35 days, h should be

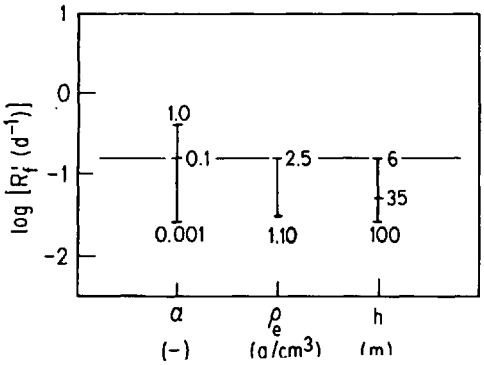

Figure 10. Sensitivity of R'_f to variations in coagulation parameter values. The horizontal line was calculated using the parameter values indicated and for $C_p = 10^{-7}$ kg l^{-1} · $K_c^* = K_{pc} = 10^7$.

approximately 38 m for the deep ocean. In nearshore environments, bays and estuaries, h should represent the mean depth as the life of a ^{234}Th atom would probably exceed the length of time that it would take for sedimentation out of the system.

Line 1 is for Brownian coagulation/sedimentation, only, and Line 2 includes shear coagulation/sedimentation ($G = 1.0\ s^{-1}$): particle aggregation by shear is important only at $C_p > 10$ mg/l. The lines indicate the conditions such that $R'_f = B'_b + B'_{sh}$: that is, the limiting sorption rate. The line initially has a slope of 0.3 as expected from Eq. 3 and increases as the region of the shear coagulation mechanism is reached. The sensitivity of B'_b (R'_f when $f_{c/d} = 1$) to critical coagulation parameters is shown in Figure 10. The values of 0.5 (e.g., Lal, 1980; Edzwald, *et al.*, 1974), 2.5 g/cm^3 (McCave, 1974) and 6 m for α_b, α_{sh}, ρ_e and h, respectively, were used in the calculation of Lines 1 and 2 (Fig. 9a). Since none of the parameters are, themselves, functions of C_p, any change in their values will shift the coagulation rate line in a direction parallel to the solid lines. As it is likely that the values of α and ρ are maximum values and h a minimum value, this line represents an upper limit for coagulation coupled to sedimentation. With the exception of the deep sea data points, Lines 1 and 2 model the data reasonably well. In the case of the low C_p data, decreasing α or increasing h would decrease the calculated scavenging rate constant. Justification for a lower α in the deep ocean is described below in conjunction with discussions of K_d observations.

The overall transfer of Th from the dissolved phase of the filterable particle fraction must include the partitioning of Th between solution and colloids; more specifically, $f_{c/d}$ must be determined. Unfortunately, the mass (C_p^*) and adsorption characteristics of colloids (K_c^*) in the oceanic water column are unknown. However, it is possible to use equilibrium K_d data to estimate the relative magnitude of these parameter's values.

Figure 11 shows log K_d as a function of log C_p for ^{230,234}Th and ^{7}Be data. At low

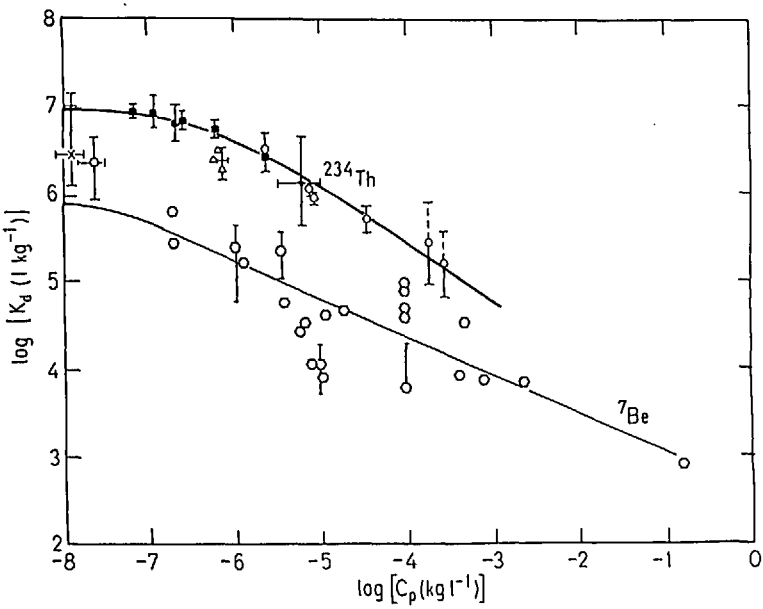

Figure 11. Log K_d versus log C_p for ^{230,234}Th and ^{7}Be. Data: for Th: Coale and Bruland, 1985; McKee *et al.*, 1984; Santschi *et al.*, 1979; Minagawa and Tsunogai, 1980; after Honeyman *et al.*, 1988; for ^{7}Be; Li *et al.*, 1984; Nyffeler *et al.*, 1984; Hawley *et al.*, 1986 Buchholtz, 1987; Bloom and Crecelius, 1983; Olson *et al.*, 1984; after Honeyman and Santschi, 1988. Relationships among master variables for model calculations correspond to those of Figure 9.

values of C_p, log K_d for Th appears to be independent of C_p. As C_p increases, log K_d decreases monotonically with C_p. Equation B14 describes the relationship between K_{pc}, K_c^*, C_p^* and K_d for a system containing two particle-size classes. For conditions such that the product of K_c^* and C_p^* is small compared to 1 (i.e., less than 0.05), K_d is constant and equal to K_{pc}. Therefore, Figure 11 indicates that K_{pc} for Th $\sim 10^{6.8}$ to $10^{7.0}$. As C_p increases C_p^* will also increase and the term $K_c^* C_p^*$ becomes much larger than about 0.05. At this point, K_d will have a reciprocal dependence on C_p, the exact relationship depending on the functional relationship between C_p^* and C_p. Since K_c^* and K_{pc} are assumed to be constant, the slope of the log K_d versus log C_p plot (for $C_p > 10^{-6}$ kg/L) indicates that $C_p^* = f(C_p^{0.7})$. This is also the slope suggested by Morel and Gschwend (1987) for the relationship between the "microparticles" and "macroparticles" in Gschwend and Wu's (1985) data. If it is assumed that $K_c^* = K_{pc}$, then it follows that log $C_p^* = 0.7$ log $C_p - 2.6$. Such a relationship between C_p^* and C_p includes the particle-concentration ratio needed to model Nyffeler *et al.*'s (1984) data for marine sediments and is in the proximity of that for the lake and stream sediments described by Gschwend and Wu (1985).

One aspect of the Th data shown in Figure 11 that needs to be reconciled to model

calculations is the lower measured K_d, relative to the apparent trend in the data and to the model calculations, for the very low particle concentrations, C_p, in the deep sea. The most straightforward explanation is that the deep sea particles are different in character (size, composition) from those near shore or in the upper reaches of the water column. The most likely agent is variations in DOC among different oceanic regimes. For example, the prediction put forth by Nash and Choppin (1980) about the almost complete association of Th nuclides with dissolved humic and fulvic acid colloids might also be reflected in the observations by Wahlgren *et al.* (1982) on the inverse correlation of K_d values for Th with DOC concentrations in freshwater lakes. For oceanic environments, Huh and Beasley (1987) and Cochran *et al.* (1987) independently reported lower fractions of ^{230}Th and ^{232}Th associated with filterable particles from the upper 500 m than from below that depth. This is the region where DOC concentrations are also much higher (e.g., Sugimura and Suzuki, 1988) suggesting partial association of Th with DOC. A higher concentration of DOC in deep ocean water would produce a relatively weaker K_d. Higher concentrations of DOC would also tend to strongly decrease values for the α-factor (see reviews in Ali *et al.*, 1984 or Weilemann, 1986) and K_ds for Th due to complex formation with soluble organic complexes (Wahlgren and Orlandini, 1982) while possibly also changing the C_p^*/C_p ratio.

It is also interesting to note that for a given particle-size distribution, the C_p at which K_d becomes a function of C_p will depend on the sorption characteristics of the metal, as represented by K_c^*. This facet of the model is explored in Table 3. C_p^{crit} is the particle concentration at which $K_c^* \cdot C_p^* = 0.05$. The higher the K_c^*, the more sensitive is the calculated K_d to variations in C_p. In contrast to Th, the measured K_d for many metals may be relatively independent of particle concentration until high (e.g., coastal zone) concentrations are reached.

The dashed line in Figure 9a includes both the coagulation rate and the solution/colloid partitioning of Th. The solid and dashed lines diverge by the factor $f_{c/d}$. The determination of $f_{c/d}$ is based upon $\log C_p^* = 0.7 \log C_p - 2.6$. When $f_{c/d}$ is equal to 1, the rate constant is governed solely by the coagulation/sedimentation rate and the lines converge. Under these conditions, Th is acting as an *in situ* "coagulometer."

Figure 9b shows the postulated distribution of Th species as a function of C_p for the same set of data and model calculations used in Figure 9a. The line for $f_{c/d}$ indicates that, for Th, the association of Th with the colloidal fraction dominates the "dissolved" Th pool at moderately high C_p.

The model estimate of log K_d versus log C_p (Fig. 11) for Th sorption on marine particles may be derived by two different approaches: equilibrium and kinetic formulations. The equilibrium approach has been described above. K_d represents the ratio of Th isotope activities in the filterable particle (f_{pc}) and "dissolved" ($f_c + f_d$) pools: $K_d = K_{pc}/(1 + K_c^* \cdot C_p^*) = f_{pc}/((f_c + f_d) \cdot C_p)$.

Table 3. Estimation of particle concentration, C_p^{crit}, at which K_d becomes independent of C_p. Conditions: $\log C_p^* = 0.7 \log C_p - 2.6$; $K_c^* = K_{pc}$; Criteria for C_p^{crit}: $K_c^* \cdot C_p^* = 0.05$.

$\log [K_c^*$ (l/kg)]	Representative metals	$\log [C_p^*$(kg/l)]	$\log [C_p^{crit}$(kg/l)]
7	Th	−8.3	−8.1
6	Fe, Sn, Al	−7.3	−6.7
5	Zn, Be, Mn	−6.3	−5.3
4	Mn, Co	−5.3	−3.8
3	Cs, Sb, Se	−4.3	−2.4
2	Cd, Ba	−3.3	−1.0

The alternative description follows from the kinetic approach of Nyffeler *et al.* (1984) in which K_d is expressed in terms of a ratio of rate constants:

$$K_d = \frac{R_f C_p^{\phi}}{R_r} \cdot \frac{1}{C_p} = \frac{R_f'}{R_r} \cdot \frac{1}{C_p} \tag{11}$$

where $R_f' = f(C_p^{\phi})$. At high C_p, ϕ approaches 0.3, i.e., the exponential coefficient for the dependency of B_b' on C_p. At low C_p, ϕ approaches 1.0. From Eq. 11, $\log K_d$ is proportional to $(\phi\text{-}1) \cdot \log C_p$. At low C_p, K_d is independent of C_p (the slope of $\log K_d$ versus $\log C_p$ is zero). As the sorption rate constant approaches B_b', ϕ approaches 0.3 and $\log K_d$ versus $\log C_p$ takes on a slope of $(0.3 - 1)$ or -0.7. The model calculations were made with the assumption that R_r is independent of C_p. The value of R_r required to fit the calculations to the Th data was 0.04 d^{-1}. It is the value required to achieve correspondence between equilibrium kinetic and formulations of K_d (Eqs. 8 and 11). This value is in agreement with values from Narragansett Bay (P. Santschi, unpublished data: $R_r = 0.004 - 0.07$ d^{-1}), marine particles from sediment traps (Nyffeler *et al.*, 1984: $R_r = 0.04 - 0.14$ d^{-1}) and Puget Sound (Jannasch *et al.*, 1988: $R_r = 0.03$ d^{-1}). It is also not much higher than the values calculated for deep sea suspended particles (Bacon and Anderson, 1982: $R_r = 0.004$ to 0.017 d^{-1}; Nozaki *et al.*, 1981: $R_r = 0.018$ d^{-1}).

The effect of particle concentration on K_d for ^{7}Be is also shown in Figure 11. The data, taken from the literature, are predominantly for freshwater environments although oceanic and laboratory data for natural particles are included. As in the case of the Th data, a reciprocal relationship exists between K_d and C_p: the trend of the data indicates that $C_p^* \approx f(C_p^{0.5})$, although there is significant scatter in the data. The model line was calculated from the assumption that $K_c^* = K_{pc} = 10^6$ and that $\log C_p^* = 0.5 \log C_p - 2.3$; however, given the scatter in the Be data, it would be difficult to argue that the suggested square root dependence is significantly different than the $C_p^{0.7}$ dependency proposed for the marine environments using the thorium data. These data do suggest, however, that the particle size spectrum of freshwater environments may be different than that of marine systems.

6. The Brownian-pumping model: criticisms and implications

One of the main objectives of geochemistry has been to describe the behavior of elements in natural systems from a knowledge of their fundamental physico/chemical properties. Over the last decade, surface coordination chemistry has enjoyed remarkable success at describing the fundamental interactions occurring at the particle-solution interface. Some of the debate over the significance of anomalous metal behavior has been posed in terms of a conflict between experimentalists and theorists: the former accused of invoking ad hoc mechanisms and the latter maintaining that chemical thermodynamic models of the particle/solution interface remain valid. However, the Brownian-pumping model indicates that metal behavior in natural systems is the consequence of tightly-coupled processes: chemical equilibrium and physico-chemical interactions between particles. An implication of the model for metal sorption proposed in this paper is that although surface coordination chemistry provides a useful starting point for understanding the behavior of the group of metals which are subject to "hydrolytic" scavenging, it may, alone, be insufficient. A key aspect of the metal-behavior puzzle is the distribution of submicron particles and their chemical and physical behavior.

The role of particle aggregation in metal scavenging was originally postulated to explain small scavenging rate constants. However, other explanations such as mass transport limitations or kinetically-hindered exchange have also been invoked as the controlling process. Unfortunately, the type of model that would seem to be most appropriate for hydrolytic scavenging- transport coupled to a first-order (or pseudo first-order) reversible reaction- has a rate law of the mathematical form that can also be derived from the case of physical non-equilibrium containing linear diffusion and a linear equilibrium isotherm (e.g., Nkedi-Kizza *et al.*, 1984). In other words, the two cases are mathematically equivalent and distinctions between them cannot be made purely on the basis of correspondence of the data to one of the simple rate laws.

The rate law proposed here for Brownian pumping is also, by itself, insufficient to unequivocally distinguish between other processes such as chemical kinetics or mass transport. Direct experimental evidence linking particle aggregation and metal behavior is needed to distinguish sorption control by coagulation reactions from control by diffusion of the sorbate through surface films or pore spaces (e.g., Enfield *et al.*, 1976; Epstein, 1983; Wu and Gschwend, 1986) or, in the case of radionuclides, from slow isotopic exchange (e.g., Johnston, 1977).

The advantage of the model proposed in this paper is that it provides a framework for interpreting a range in observations of thorium behavior. In addition, not only does it yield a satisfying rational for calculated Th scavenging rates, it also, without modification, can be extended to other metals of interest (for example, through K_d/k_f correlations). In this sense, the model is "predictive," although its usefulness is largely restricted to those metals which are scavenged as a consequence of adsorption. The

model provides a specific context within which sorption studies can be tested and refined.

It is also clear that the behavior of particles in natural systems is far more complicated than is suggested by the sedimentation equations. It is likely, for example, that conditions in oceans or estuaries change relatively rapidly and thereby operate against the establishment of the characteristic removal rate regimes described by Eq. 1. The phenomenological model of particle dynamics used here, the transfer of fine particles through the particle-size distribution by coagulation and their eventual removal by sedimentation, is not realistic in its description of the true life of particles. However, the quantitative aspects presented here do provide a starting point for further development of more specific models of scavenging which include particle dynamics.

One further consequence of the tight coupling of adsorption and particle aggregation may be the need to define a standard reference state for experimental investigations of metal/particulate interactions, one in which the physical state of particles is explicitly considered. For example, if the particle-concentration effect is in fact the consequence of particle-particle interactions or colloidal "impurities" then the determination of intrinsic complexation constants for metal adsorption and their intercomparison may require "standard" conditions such as: (1) a monodispersed system; (2) a standard particle size; (3) a specified particle concentration; and (4) electrolyte solutions "scrubbed" of particulate impurities to a standard level.

7. Summary

The Brownian-pumping model presented in this paper describes the transport of truly dissolved metals to a filterable particle fraction via colloidal intermediates. Phenomenologically, the model consists of two steps: (1) rapid equilibration of dissolved metal species with particle surface sites, both on colloids and in the filterable-particle fractions and (2) slower aggregation of colloids with larger particles. Step 1 is adsorbate specific while step 2 (coagulation) is, for systems with low metal/particle ratios, independent of adsorbate type. Such a decoupling of a metal's chemical and physical behavior indicates that Th data may be useful in predicting the behavior of other metals of interest.

Conclusions of this work are:

(i) Metal behavior which is seemingly at odds with adsorption theory is the result of the physical and chemical behavior of particles in an operationally-defined "dissolved" phase;

(ii) Particle aggregation is the rate determining kinetic step: measured sorption rates are the consequence of rapid absorption of metal species onto colloidal or sub-micron particles coupled to the slower aggregation of these particles with those particles in the filterable-size class;

(iii) The exponential dependency of sorption rate constants on particle concentration is consistent with the functional dependencies of aggregation rate and particle/solution partitioning on C_p;

(iv) The reciprocal dependence of K_d on C_p, the so-called "particle-concentration effect," is likely due to the presence of metal-adsorbing colloids which are non-filterable: (a) this effect is mitigated at very low C_p; (b) at higher C_ps, the relationship between K_d and C_p provides information about the relative distribution of colloids and larger, filterable particles;

(v) $C_p^* = f(C_p^\phi)$ where for oceans, estuaries, and perhaps freshwater systems, $0.4 < \phi < 0.7$;

(vi) It is possible that many of the intrinsic constants for metal sorption reported in the literature may be "weaker" than the true value because of colloids in what was assumed to be the "dissolved" phase;

(vii) Rapid adsorption coupled to slower particle aggregation provides a mechanistic explanation for extending information about Th to other metals of interest, for example, as in the empirical correlations between K_d and k_f (Jannasch *et al.*, 1988) and K_d versus C_p;

(viii) The Brownian-pumping model also suggests that Th, or other strongly-adsorbing metals, may be useful as *in situ* "coagulometers," either at relatively high particle concentrations or when the ratio of colloids to filterable particles is known. Thus, ^{234}Th sorption, at particle concentrations greater than about 5 mg/l, is occurring at the rate of particle aggregation and removal.

(ix) Results presented in this paper indicate that system *scale* is critical when extrapolating laboratory data to natural environments. This includes the effect of C_p on rate and extent of sorption (due to the dependency of C_p^* on C_p) and the size of the uniformly mixed column of water when coupling coagulation and sedimentation (i.e., h).

(x) Finally, the results presented in this paper indicate that physical effects such as particle-particle interactions largely control the behavior of many metals in heterogeneous systems and that such effects need to be elucidated before the fate and transport of metals in natural systems can be well-understood.

Acknowledgments. The work described in this paper was carried out at the Swiss Institute of Water Resources and Water Pollution Control, CH-8600 Dubendorf, Switzerland, which also provided some logistical and financial support for this project. Daniel Sutter manufactured and characterized the goethite used in this study, and Klaus Farrenkothen helped with many aspects of the experimental study. We thank Jim Murray, Laurie Balistrieri, Hans Jannasch, Michael Bacon and three anonymous reviewers for their thoughtful comments on earlier versions of this manuscript and Beatrice Schwertfeger for typing and editing. This material is based in part upon work supported by the Swiss National Science Foundation and by Texas A&M University, by the Texas Advanced Research Programs (Grant #4697).

APPENDIX A

Symbol definition

α = collision efficiency factor (−)
$\hat{B}$ = pseudo first order overall coagulation/sedimentation rate coefficient (t^{-1})
= $-B_{ds}C_p^{1.3} - B_{sh}C_p^{0.9} - B_bC_p^{0.3}$
B_b = Brownian coagulation coefficient ($mg^{-0.3}l^{0.3}s^{-1}$)
B'_b = pseudo-first order Brownian coefficient (s^{-1})
B_{sh} = Shear coagulation coefficient ($mg^{-0.9}l^{0.9}s^{-1}$)
B'_{sh} = pseudo-first order shear coefficient (s^{-1})
C_p = mass concentration of filterable particles (kg/l)
C_p^* = mass concentration of colloids (kg/l)
f_c = fraction of total metal associated with colloids = Me_c/Me_T
$f_{c/d}$ = fraction of "dissolved" metal associated with colloids
f_{pc} = fraction of total metal associated with filterable particles Me_{pc}/Me_T
G = Shear rate (s^{-1})
Γ = adsorption density (moles adsorbed/mass particles)
K_c^* = equilibrium association constant for colloidal particles (l/kg)
K_d = equilibrium distribution coefficient (l/kg)

$$= \frac{Me_{pc}}{\{Me_c + Me_d\}} \cdot \frac{1}{C_p} = \frac{Me_{pc}}{\tilde{M}e_d} \cdot \frac{1}{C_p}$$

k_f = pseudo first order sorption rate constant (t^{-1})
K_{pc} = equilibrium association constant for filterable particles (l/kg)
Me_{ads} = total adsorbed metal = $Me_{pc} + Me_c$ (m)
Me_c = metal associated with colloids (m)
Me_d = truly dissolved metal (m)
$\tilde{M}e_d$ = operationally defined dissolved metal $Me_c + Me_d$ (m)
Me_{pc} = metal associated with filterable particles (m)
Me_T = total metal = $Me_{pc} + Me_c + Me_d$ (m)
Q_d = non-equilibrium distribution coefficient (l/kg) $Q_d \rightarrow K_d$ as $t \rightarrow \infty$
R'_f = pseudo first order sorption rate constant (t^{-1})

APPENDIX B

Relationships among master variables

$$Me_T = Me_c + Me_{pc} + Me_d \tag{B1}$$

If

$$K_c^* = \frac{Me_c}{Me_d} \cdot \frac{1}{C_p^*} \quad \text{and} \quad K_{pc} = \frac{Me_{pc}}{Me_d} \cdot \frac{1}{C_p} \tag{B2}$$

then

$$Me_c = K_c^* \cdot C_p^* \cdot Me_d \quad \text{and} \quad Me_{pc} = K_{pc} \cdot C_p \cdot Me_d \tag{B3}$$

$$Me_T = Me_d\{K_c^* \cdot C_p^* + K_{pc} \cdot C_p + 1\} = Me_d \cdot \Sigma \tag{B4}$$

$$f_{pc} = \frac{Me_{pc}}{Me_T} = \frac{K_{pc} \cdot C_p}{\Sigma} \tag{B5}$$

$$f_c = \frac{Me_c}{Me_T} = \frac{K_c^* \cdot C_p^*}{\Sigma} \tag{B6}$$

$$f_d = \frac{Me_d}{Me_T} = \frac{1}{\Sigma} \tag{B7}$$

$$f_{c/d} = \frac{f_c}{f_c + f_d} = \frac{K_c^* \cdot C_p^*}{K_c^* \cdot C_p^* + 1} \tag{B8}$$

The distribution coefficients, Q_d and K_d are *apparent* distribution coefficients since the operationally-defined dissolved phase contains both truly-dissolved and colloid-associated metal species. Considering an equilibrium distribution

$$K_d = \frac{Me_{pc}}{\tilde{M}e_d} \cdot \frac{1}{C_p} = \frac{Me_{pc}}{(Me_c + Me_d)} \cdot \frac{1}{C_p} \tag{B9}$$

Thus

$$K_d \longrightarrow K_{pc} \text{ as } Me_c \longrightarrow 0$$

$$Me_{pc} = K_d \cdot \tilde{M}e_d \cdot C_p = K_{pc} \cdot Me_d \cdot C_p \tag{B10}$$

Eqs. B1 and B5 may also be written in terms of operational parameters

$$Me_T = Me_{pc} + \tilde{M}e_d = \tilde{M}e_d(1 + K_d \cdot C_p) \tag{B11}$$

$$f_{pc} = \frac{Me_{pc}}{Me_T} = \frac{K_d \cdot C_p \cdot \tilde{M}e_d}{\tilde{M}e_d(1 + K_d \cdot C_p)} \tag{B12}$$

The ratio of truly dissolved metal to apparently dissolved metal is

$$\frac{Me_d}{\tilde{M}e_d} = \frac{f_d}{f_d + f_c} = \frac{1}{1 + K_c^* \cdot C_p^*} \tag{B13}$$

The distribution coefficient, K_d, is related to K_{pc} by

$$K_d = \frac{f_{pc}}{f_c + f_d} \cdot \frac{1}{C_p} = \frac{K_{pc}}{1 + K_c^* \cdot C_p^*} \tag{B14}$$

Thus,

$$K_d \longrightarrow K_{pc} \text{ as } K_c^* \cdot C_p^* \tag{B15}$$

becomes < 0.05.

For conditions where $K_c^* \cdot C_p^* \gg 0.05$, the relationship between K_d and C_p depends

on the ratio of C_p^* to C_p. If $K_c^* \cdot C_p^* \gg 1.0$ then

$$K_d = \left(\frac{K_{pc}}{K_c^*}\right)\frac{1}{C_p^*} \tag{B16}$$

$$\log K_d = -\log C_p^* + \log (K_{pc}/K_c^*) \tag{B17}$$

APPENDIX C

Kinetic analysis of ^{228}Th sorption

Kinetics is described using the general mathematical development for a reversible first-order reaction (e.g., Levenspiel, 1972). More specifically, we are interested in the transfer of radioactive species on colloids in the non-filterable fraction to the filterable-particle fractions.

$$D \underset{k_r}{\overset{k_f}{\rightleftharpoons}} P \tag{C1}$$

where D and P represent "dissolved" and "particulate" ^{228}Th activities (e.g., dpm l^{-1}), respectively, and k_f and k_r are pseudo-first order rate coefficients (time^{-1}).

$$\frac{dP}{dt} = -\frac{dD}{dt} = D_o \cdot \frac{dX_D}{dt} \tag{C2}$$

and $X_D = D_o - D_t/D_o$ (the reaction extent). D_o and D_t represent "dissolved" ^{228}Th activities at $t = 0$ and $t = t$, respectively.

$$\frac{dP}{dt} = k_f \cdot D - k_r \cdot P \tag{C3a}$$

$$= k_f(D_o - D_o \cdot X_D) - k_r(D_o \cdot I + D_o \cdot X_D) \tag{C3b}$$

I is the initial ($t \approx o$) particle/solution activity ratio and represents the "instantaneous" initial partitioning of the metal adsorbate between the "dissolved" phase and particle cluster. Thus,

$$I = \frac{P_o}{D_o} \tag{C4}$$

The initial $Q_d(Q_d^\circ)$ is related to I by

$$Q^\circ = \frac{P_o}{D_o} \cdot \frac{1}{C_p} \cdot \frac{I}{C_p} \tag{C5}$$

The equilibrium $K_d(Q_d)$ as $t \rightarrow \infty$

$$K_d = \frac{P_e}{D_e} \cdot \frac{1}{C_p} = \left\{\frac{1 + \bar{X}_D}{1 - \bar{X}_D}\right\} \cdot \frac{1}{C_p} = \frac{k_f}{k_r} \cdot \frac{1}{C_p} \tag{C6}$$

where the subscript "e" indicates activities at equilibrium and $\bar{X}_D$ the reaction extent at equilibrium (i.e., as $t \rightarrow \infty$). Combining (C6) with (C3) yields (C7)

$$\frac{dX_D}{dt} = k_f(1 - X_D) - k_r(I + X_D) = \frac{k_f(I + 1)}{I + X_D} \cdot (\bar{X}_D - X_D) \tag{C7}$$

Integrating C7 yields:

$$-\ln\left\{1 - \frac{\bar{X}_D}{X_D}\right\} = -\ln\left\{\frac{D_t - D_e}{D_o - D_e}\right\} = \left\{\frac{I + 1}{I + X_D}\right\} k_f \cdot t \tag{C8}$$

REFERENCES

Ali, W. and C. P. O'Melia. 1984. Colloid stability of particles in lakes: measurement and significance. Water Sci. Technol., *17*, 701–712.

Amirtharajah, A. 1985. The interface between filtration and backwashing. Water Res., *19*, 581–588.

Bacon, M. and R. Anderson. 1982. Distribution of thorium isotopes between dissolved and particulate forms in the deep sea. J. Geophy. Res., *87*, 2045–2056.

Bacon, M., C.-H. Huh, A. Fleer and W. G. Deuser. 1985. Seasonality in the flux of natural radionuclides and plutonium in the deep Sargasso Sea. Deep-Sea Res., *32*, 273–286.

Balistrieri, L. S., P. G. Brewer and J. W. Murray. 1981. Scavenging residence times of trace metals and surface chemistry of sinking particles in the deep ocean. Deep-Sea Res., *28*, 101–121.

Balistrieri, L. S. and J. W. Murray. 1981. The surface chemistry of goethite (α—FeOOH) in major ion seawater. Amer. J. Sci., *281*, 788–806.

Bloom, N. and E. A. Crecelius. 1983. Solubility behavior of atmospheric ^{7}Be in the marine environment. Mar. Chem., *12*, 323–331.

Buchholtz, M. 1987. Radioisotope mobility across the sediment water interface in the deep sea. Ph.D. thesis, Columbia University, NY.

Buchholtz, M., P. H. Santschi, and W. S. Broecker. 1986. Comparison of radiotracer K_d values from batch equilibrium experiments with *in situ* determinations in the deep sea using the Manop Lander: the importance of geochemical mechanisms in controlling ion uptake and migration, *in* Application of Distribution Coefficients to Radiological Assessment Models, T. H. Sibley and C. Myttenaee, eds., Elsevier Applied Science Publishers London, 192–206.

Buddemeier, R. W. and J. R. Hunt. 1988. Transport of colloidal contaminants in groundwater: Radionuclide migration at the Nevada Test Site. Appl. Geochem., *3*, 535–548.

Cacheris, W. P. and G. R. Choppin. 1987. Dissociation kinetics of thorium-humate complex. Radiochemica Acta, *42*, 185–190.

Coale, K. H. and K. W. Bruland. 1985. ^{234}Th: ^{238}U disequilibria within the California Current. Limnol. Oceanogr. *30*, 22–33.

Cochran, J. K., E. A. Carey, E. A. Sholkovitz, and L. D. Surprenant. 1986. The geochemistry of uranium and thorium in coastal marine sediments and sediment-pore waters. Geochim. et Cosmochim. Acta, *50*, 663–680.

Davis, J. A., R. O. James and J. O. Leckie. 1978. Surface ionization and complexation at the oxide/water interface. J. Colloid Interf. Sci., *63*, 480–499.

Diamadopoulos, E. and D. R. Woods. 1984. The effect of filter pore size on the evaluation of aluminium coagulants to remove fulvic acid from water. Water Res., *11*, 1455–1459.

Di Toro, D. M., J. D. Mahony, P. R. Kirchgraber, A. L. O. Bryne, L. R. Pasquale and D. C. Piccirilli. 1986. Effects of non-reversibility, particle concentration and ionic strength on heavy metal adsorption. Environ. Sci. Technol., *20*, 50–61.

Edzwald, J. K., J. C. Upchurch, and C. R. O'Melia. 1974. Coagulation in estuaries. Environ. Sci. Technol., *8*, 58–63.

Enfield, C. E., C. C. Harlin, Jr and B. E. Bledsoe. 1976. Comparison of five kinetic models for orthophosphate reactions in mineral soils. Soil Sci. Soc. Am. J., *40*, 243–249.

Epstein, G. B. 1983. Isothermal diffusion of Eu(III) and Th(IV) in deep sea sediments: experimental results and numerical model. M.S. thesis, University of Rhode Island, Kingston, RI.

Farley, K. J. 1984. Sorption and sedimentation as mechanisms of trace metal removal. Ph.D. Thesis, Massachusetts Institute of Technology, Cambridge, MA.

Farley, K. J. and F. M. M. Morel. 1986. Role of coagulation in sedimentation kinetics. Environ. Sci. Technol., *20*, 187–195.

Friedlander, S. K. 1977. Smoke, Dust and Haze, John Wiley and Sons, NY, 317 pp.

—— 1960a. On the particle-size spectrum of atmospheric aerosols, J. Meterol., *17*, 373–374.

—— 1960b. Similarity considerations for the particle-size spectrum of a coagulating, sedimenting aerosol., J. Meteorol., *17*, 479–483.

Gschwend, P. M. and S.-C. Wu. 1985. On the constancy of sediment-water partitioning coefficients of hydrophobic organic pollutants. Environ. Sci. Technol., *19*, 90–96.

Hawley, N., J. A. Robbins and B. J. Eadie. 1986. The partitioning of ^{7}Be in fresh water. Geochim. et Cosmochim. Acta, *50*, 1127–1132.

Hayes, K. F. and J. O. Leckie, 1986. Mechanism of lead-ion adsorption at the geothite-water interface, *in* Geochemical Processes at Mineral Surfaces, J. A. Davis, and K. F. Hayes, eds., American Chemical Society Symposium Series No. 323: Washington D.C., Chapter 7.

Higgo, J. J. W. and L. V. C. Rees. 1986. Adsorption of actinides by marine sediments: effect of the sediment/seawater ratio on the measured distribution coefficient. Environ. Sci. Technol., *20*, 483–490.

Hoffman, M. 1981. Thermodynamic, kinetic, and extrathermodynamic considerations in the development of equilibrium models for aquatic systems. Environ. Sci. Technol., *15*, 345–353.

Hohl, H. and W. Stumm. 1976. Interaction of Pb^{2+} with hydrous γ-Al_2O_3. J. Colloid. Interf. Sci., *55*, 281–288.

Honeyman, B. D., L. S. Balistrieri and J. W. Murray. 1988. Oceanic trace metal scavenging: the importance of particle concentration. Deep-Sea Res., *35*, 227–246.

Honeyman, B. D. and P. H. Santschi. 1988. Critical review: Metals in aquatic systems. their scavenging residence times from laboratory data remains a challenge. Environ. Sci. Technol., *22*, 862–871.

Huh, C.-A. and T. J. Beasley. 1987. Profiles of dissolved and particulate thorium isotopes in water columns of central Southern California. Earth Planet. Sci. Lett., *85*, 1–10.

Hunt, J. R. 1980. Prediction of oceanic particle-size distributions from coagulation and sedimentation mechanisms, *in* Particles in Water, M. C. Kavanaugh and J. O. Leckie, (ed.), American Chemical Soc. Advances in Chemistry Series No. 189, 243–257.

—— 1982. Particle dynamics in seawater: implications for predicting the fate of discharged particles. Environ. Sci. Technol., *16*, 303–309.

Hunt, J. R. and J. D. Pandya. 1984. Sewage sludge coagulation and settling in seawater. Environ. Sci. Technol., *18,* 119–121.

Hunter, K. A., D. J. Hawke and L. K. Choo. 1988. Equilibrium adsorption of thorium by metal oxides in marine electrolytes. Geochim et Cosmochim. Acta., *52,* 627–636.

Jannasch, H. W., B. D. Honeyman, L. S. Balistrieri and J. W. Murray. 1988. Kinetics of trace element uptake by marine particles. Geochim. et Cosmochim. Acta., *52,* 567–577.

Jeffery, D. J. 1982. Aggregation and breakup of clay flocs in turbulent flow. Advances in Colloid and Interface Science, *17,* 213–218.

Johnson, B. D. and P. J. Wangersky. 1985. Seawater filtration: particle flow and impact considerations. Limnol. Oceanogr., *30,* 966–971.

Johnston, F. J. 1977. Isotopic exchange processes, *in* Radiotracer Techniques and Applications, E. A. Evans and M. Nurawatsu, eds., Marcel Dekker, Inc., NY, 405–456.

Kepak, F. 1977. Behavior of carrier-free radionuclides, *in* Radiotracer Techniques and Applications, A. Evans and M. Muramatsu, eds., Marcel Dekker, Inc. NY, Chapter 8.

Lal, D. 1980. Comments on some aspects of particulate transport in the oceans. Earth and Planet. Sci. Lett. *49,* 520–527.

Levenspiel, O. 1972. Chemical Reactor Engineering, 2nd Edition, John Wiley and Sons, NY, 578 pp.

Li, W. C., D. E. Armstrong, J. D. H. Williams, R. F. Harris, and J. K. Syers. 1972. Rate and extent of inorganic phosphate exchange in lake sediments. Soil Sci. Soc. Am. Proc., *36,* 279–285.

Li, Y.-V., L. Burkhardt, M. Buchholtz, P. O'Hara, and P. H. Santschi. 1984. Partitioning of radiotracers between suspended particles and seawater. Geochim. et Cosmochim. Acta., *48,* 2011–2019.

Mackay, D. and B. Powers. 1987. Sorption of hydrophobic chemicals from water: a hypothesis for the mechanism of the particle concentration effect. Chemosphere, *16,* 745–757.

Mayer, L. M. 1982. Aggregation of colloidal iron during estuarine mixing: kinetics, mechanism and seasonality. Geochim. et Cosmochim. Acta, *46,* 2527–2535.

McDowell-Boyer, L. M., J. R. Hunt, and N. Sitar. 1986. Particle transport through porous media. Water Res. Res. *22,* 1901–1921.

McCave, I. N. 1984. Size spectra and aggregation of suspended particles in the deep ocean. Deep-Sea Res., *31,* 329–352.

McKee, B. A., D. J. DeMaster, and C. A. Nittrouer. 1986. Temporal variability in the partitioning of thorium between dissolved and particulate phases on the Amazon shelf: implications for the scavenging of particle-reactive species. Con. Shelf Res., *6,* 87–106.

—— 1984. The use of $^{234}Th/^{238}U$ disequilibrium to examine the fate of particle-reactive species on the Yangtze. Cont. Shelf, *68,* 431–442.

Minagawa, M. and S. Tsunogai. 1980. Removal of ^{234}Th from a coastal sea: Funka Bay, Japan. Earth Planet. Sci. Lett., *47,* 51–64.

Moore, R. M. and G. E. Millward. 1988. The kinetics of reversible Th reactions with marine particles. Geochim. et Cosmochim. Acta, *52,* 113–118.

Morel, F. M. M. and P. M. Gschwend. 1987. The role of colloids in the partitioning of solutes in natural waters, *in* Aquatic Surface Chemistry: Chemical Processes at the Particle-Water Interface. W. Stumm, ed., John Wiley, NY. Chapter 15.

Morel, F. M. M. and J. M. Hudson. 1986. The geobiological cycle of trace elements in aquatic systems: Redfield revisited, *in* Chemical Processes in Lakes. W. Stumm, ed., Wiley-Interscience, NY. Chapter 12.

Nash, K. L. and G. R. Choppin. 1980. Interaction of humic and fulvic acids with Th(IV). J. Inorg. Nucl. Chem., *42,* 1045–1050.

Niven, S. E. H. and R. M. Moore. 1988. Effect of natural colloidal matter on the equilibrium adsorption of thorium in seawater, *in* Radionuclides: A Tool for Oceanography. J. Guary *et al.*, ed. Elsevier, 111–120.

Nkedi-Kizza, P., W. Biggar, H. M. Selim, M. T. van Genuchten, P. J. Wierenga, J. M. Davidson, and D. R. Neilson. 1984. On the equivalence of two conceptual models for describing ion exchange during transport through an aggregated oxisol. Water Res. Res., *20,* 1123–1130.

Nozaki, Y., Y. Horibe and H. Tsubota. 1981. The water column distributions of thorium isotopes in the western North Pacific. Earth Planet. Sci. Lett., *54,* 203–216.

Nozaki, Y., H.-S. Yang, and M. Yamada. 1987. Scavenging of thorium in the ocean. J. Geophys. Res., *87,* 2045–2056.

Nyffeler, U. P., Y.-H. Li, and P. H. Santschi. 1984. A kinetic approach to describe trace element distribution between particles and solution in natural systems. Geochim. et Cosmochim. Acta, *48,* 1513–1522.

Nyffeler, U. P., P. H. Santschi, and Y.-H. Li. 1986. The relevance of scavenging kinetics to modeling of sediment-water interactions in natural waters. Limnol. Oceanogr., *31,* 277–292.

Olsen, C. R., I. L. Larsen, R. H. Brenster, N. H. Cutshall, R. F. Bopp, and H. J. Simpson. 1984. A geochemical assessment of sedimentation and contaminant distributions in the Hudson-Raritan estuary. NOAA Tech. Rep. NOS OMS 2, National Technical Information Service, Springfield, VA.

Santschi, P. H., D. M. Adler, M. Amdurer, Y.-H. Li, and J. Bell. 1980. Thorium isotopes as analogues for "particle-reactive pollutants. Earth Planet. Sci. Lett., *47,* 327–335.

Santschi, P. H., M. Amdurer, D. Adler, P. O'Hara, Y.-H. Li, P. Doering. 1987. Relative mobility of radioactive trace elements across the sediment-water interface in the MERL model ecosystems of Narragansett Bay. J. Mar. Res., *45,* 1007–1048.

Santschi, P. H., Y.-H. Li, D. M. Adler, M. Amdurer, J. Bell and U. P. Nyffeler. 1983. The relative mobility of natural (Th, Pb and Po) and fallout (Pu, Am, Cs) radionuclides in the coastal marine environment: results from model ecosystems and Narragansett Bay. Geochim. et Cosmochim. Acta, *47,* 201–210.

Santschi, P. H., Y.-H. Li, and J. Bell. 1979. Natural radionuclides in the water of Narragansett Bay. Earth Planet. Sci. Lett., *45,* 201–213.

Santschi, P. H., U. P. Nyffeler, Y.-H. Li, and P. O'Hara. 1986. Radionuclide cycling in natural waters: relevance of scavenging kinetics, *in* Sediments and Water Interactions, P. G. Syl, ed., Springer-Verlag, NY, Chapter 17.

Schindler, P. W. 1975. Removal of trace metals from the oceans: a zero order model. Thalassia Jugoslav., *11,* 101–111.

Schindler, P. W., B. Fürst, R. Dick, and P. U. Wolf. 1976. Ligand properties of surface silanol groups: I. Complex formation with Fe^{3+}, Cu^{2+}, Cd^{2+} and Pb^{2+}. J. Colloid. Interf. Sci., *55,* 469–475.

Sheppard, J. C., M. J. Campbell, T. Cheng, and J. A. Kittrick. 1980. Retention of radionuclides by mobile humic compounds and soil particles. Environ. Sci. Technol., *11,* 1349–1353.

Smoluchowski, M. 1917. Versuch einer mathematischen Theorie der Koaguationskinetik kolloider Lösungen, Z. Physik Chem., *92,* 129–169.

Sposito, G. 1986. Distinguishing adsorption from surface precipitation, *in* Geochemical processes at Mineral Surfaces, J. A. Davis, and K. F. Hayes, eds., American Chemical Society Symposium Series No. 323: Washington, D.C., Chapter 11.

Sugimura, Y. and Y. Suzuki. 1988. A high-temperature catalytic oxidation method for the determination of non-volatile dissolved organic carbon in seawater by direct injection of a volatile sample. Mar. Chem., *24,* 105–131.

Tsunogai, S. and M. Minagawa. 1978. Settling model for the removal of insoluble chemical elements in seawater. Geochim. J., *12*, 483–490.

Wahlgren, M. A. and K. A. Orlandini. 1982. Comparison of the geochemical behavior of plutonium, thorium and uranium in selected North American lakes, *in* Environ. Origination of Long-lived radionuclides, Proc. IAEA Symp., Knoxville, Tennessee, IAEA-SM-257/89, Vienna, 757–725.

Wang, C. S. and S. K. Friedlander. 1967. The self-preserving particle-size distribution for coagulation by Brownian motion. II. Small particle slip correction and simultaneous shear flow. J. Colloid Interf. Sci., *17*, 170–179.

Weilenmann, U. 1986. The role of coagulation for the removal of particles by sedimentation in lakes. Ph.D. thesis, Swiss Inst. Technol., Zuerich, Switzerland.

Whitfield, M. and D. R. Turner. 1987. The role of particles in regulating the composition of seawater, *in* Aquatic Surface Chemistry, W. Stumm, ed., John Wiley and Sons, NY, Chapter 17.

Wu, S.-C. and P.M. Gschwend. 1986. Sorption kinetics of hydrophobic organic compounds to natural sediments and soils. Environ. Sci. Technol., *20*, 717–725.

Yasunaga, T. and T. Ikeda. 1986. Adsorption-desorption kinetics at the metal-oxide-solution interface studied by relaxation methods, *in* Geochemical processes at mineral surfaces, J. A. Davis, and K. F. Hayes, eds., American Chemical Society Symposium Series No. 323: Washington, D.C., Chapter 12.